PENSOFT
SENCKENBERG world of biodiversity
Leibniz Association

Preimaginal evidence further elucidates the evolutionary history of the genus *Sinobirma* Bryk, 1944 (Lepidoptera: Saturniidae)

Zhengyang Liu[1]

1 *Zhangdian District, Zibo, Shandong Province 255000, China*

https://zoobank.org/4CADCFF4-84FE-4D10-8FC5-23769DC8DEE3

Corresponding author: Zhengyang Liu (saturniidae@qq.com)

Received 23 March 2023
Accepted 26 January 2024
Published 28 March 2024

Academic Editors Anna Hundsdörfer, Andreas Zwick

Citation: Liu ZY (2024) Preimaginal evidence further elucidates the evolutionary history of the genus *Sinobirma* Bryk, 1944 (Lepidoptera: Saturniidae). Arthropod Systematics & Phylogeny 82: 201–233. https://doi.org/10.3897/asp.82.e104232

Abstract

The moth genus *Sinobirma* was reared successfully for the first time, based on specimens of *Sinobirma bouyeri* collected in the southeastern Himalayas of Tibet. Larvae were reared on the host plants *Coriaria nepalensis* and *Prunus cerasoides* in captivity in Yunnan. Morphology and biology of the ovum, larvae, and pupa of *S. bouyeri* are described in detail. The species exhibits strong gregarious behavior during all larval instars, with mature larvae of *S. bouyeri* primarily feeding at night. The larvae are black and decorated with green stripes, pupating individually in the soil. Numerous host plants known to be used by African and Asian Saturniidae were tested with larvae of this species. The first parasitoid for the genus *Sinobirma* is reported. The complete mitochondrial genome was sequenced and used to reconstruct a molecular phylogeny to test the tribal placement of *Sinobirma*. The paper provided further evidence that *Sinobirma* originated from the African mainland and reached the Himalayas through dispersal.

Key words

Africa, biogeography, China, chaetotaxy, ecology, fluorescence, Himalayas, India, mitochondrial genome, life-history, morphology, Myanmar, parasitoid, phylogeny, SEM, Urotini

1. Introduction

Despite being one of the most enigmatic members of the Asian fauna of Saturniidae, the complete life history of the genus *Sinobirma* Bryk, 1944 has remained unknown. Currently, only four taxa are included in the genus, which is now regarded as a member of Urotini, all other genera of the tribe are distributed in mainland Africa and Madagascar in contrast to the Asian *Sinobirma* (Rougerie et al. preprint). Due to the restricted and isolated occurrence of *Sinobirma* in the eastern end of the Himalayas, only a few reports and studies on the genus have been published in the past. Consequently, the biology and evolutionary history of *Sinobirma* have remained one of the largest mysteries in the study of Saturniidae so far.

Swedish entomologist René Malaise tested his famous design of an insect trap (the Malaise trap) during an expedition to northeastern Burma in 1934, specifically around Kambaiti [Kanpaikti Sub-Township (the local official spelling today)], in Kachin State of Burma, only about

1 km from the border of the Chinese province Yunnan. Using these traps and light, René and his wife Ebba Malaise collected a large number of lepidopterous specimens (Vårdal and Taeger 2011), including some new taxa in the family Saturniidae, later studied and published by Felix Bryk. This author described *Sinobirma* from the "Sino/Birma" [China/Burma] border as a subgenus of *Opodiphthera* Wallengren, 1858 (Bryk 1944), although the latter taxon is now known to be distributed only in Oceania. At the same time, the type species *Sinobirma malaisei* (Bryk, 1944) was named in honor of René Malaise, based on one female (holotype) and three males (paratypes) collected by him in Kambaiti at an elevation 2000 m in June 1934.

After half a century of silence, Bryk's taxonomic opinion was challenged. Nässig and Oberprieler (1994) studied the types of *S. malaisei* and compared them with the genera *Tagoropsis* C. & R. Felder, 1874, *Pseudantheraea* Weymer, 1892 and *Maltagorea* Bouyer, 1993. Surprisingly, the male genitalia of *S. malaisei* demonstrated a close relationship to these Afro-Madagascan genera, instead of Australasian *Opodiphthera*. *Sinobirma* was elevated by these authors to full genus status, accompanied by two evolutionary hypotheses: Either the ancestral population drifted on the insular India from eastern Gondwana and north to continental Asia (vicariance), or it originated from Africa and then colonized the Indian Subcontinent through Arabia and the Tethys Sea (dispersal). Nässig and Oberprieler (1994) preferred the former case. The paper proposed a potential plesiomorphic feature, i.e., *Sinobirma* and *Pseudantheraea* have obvious eyespots on their hindwings in common, while *Tagoropsis* and *Maltagorea* have reduced or even no hindwing eyespots. A pair of protrusions on the posterior margin of sternum A_8 was discovered only in males of *S. malaisei* and *Maltagorea auricolor* (Mabille, 1879), but unfortunately, no further specimens beyond the type series of *S. malaisei* were available for more detailed study at that time.

About 70 years after Malaise's entomological excursion, seven males and four females of *S. malaisei* were collected by Rodolphe Rougerie in Tongbinguan [sic] [Tongbiguan, Yunnan], a nature reserve near the type-locality at an elevation of 2080 m, during the nights of 12–13 June 2001. Rougerie (2003) described for the first time the female genital structures of *S. malaisei* and illustrated living adults of both genders. Based on detailed study, the 2-segmented labial palpus of adult *S. malaisei* was stated to be the same as in the genus *Tagoropsis* but unlike *Pseudantheraea* (1 segment) and *Maltagorea* (3 segments); more importantly, both *S. malaisei* and *M. auricolor* were further recognized as sharing similar and unique traits in their aedeagi and female terga A_8. Rougerie (2003) considered conservatively that a clarification of which genus is closest to *Sinobirma* among the three candidates *Tagoropsis*, *Pseudantheraea* and *Maltagorea* would significantly advance our understanding of their evolutionary history.

The record of one additional male of *S. malaisei* was reported by Vinciguerra and Racheli (2005), noted as "Binguanshan, 2500 m, near Myitkyina, June 2004, Ying et al. leg. [sic]". Although the authors regarded it to be a Burmese specimen, the name "Binguanshan" is Chinese and means "Binguan Mountain". This location may be near the record of Rougerie (2003) on the border of western Yunnan.

The genus *Sinobirma* had long been overlooked in China. Other than Zhang and Li (2011: 451) and Zhang (2012), who illustrated a live male of *S. malaisei*, no other Chinese authors mentioned the genus in their publications. The adult sizes and colors of this species look somewhat like the genus *Eupterote* Hübner, 1820 in the family Eupterotidae (monkey-moths), of which several natural habitats overlap with the distribution of *Sinobirma*. Apparently, many Chinese collectors misidentified *Sinobirma* as *Eupterote*, thereby missing the opportunity to study the former.

Based on live material from Yunnan, Rougerie et al. (2012) illustrated for the first time the ovum and L_1 larvae of *S. malaisei*. Fed with cherry plum, these larvae died soon after the first moult. Combining adult morphology, COI and 28S rRNA sequences, these authors described two new taxa: *Sinobirma myanmarensis* Naumann, Nässig & Rougerie, 2012 ("*S. malaisei* ♂♂ R" in d'Abrera 2012: 148) and *Sinobirma bouyeri* Naumann, Nässig & Rougerie, 2012, from the type-localities Chudu Razi Hills (northern Burma) and Tomi [sic] [Tongmai Village, Bomê County, Tibet], respectively.

More recently, Sondhi et al. (2021a) included photographs of live females of *S. myanmarensis* and *S. bouyeri* from northeastern India, Kigwema Village, Kohima District of Nagaland. This represents a distinct range expansion for the genus. Sondhi et al. (2021b) also illustrated a pinned female of *S. bouyeri*. Although the type series of *Sinobirma occidentalis* Naumann & Smetacek, 2023 originated from the southeastern Himalayas, the characters stated to diagnose the new taxon (Naumann and Smetacek 2023) were minor and within the range of variation I observed, including imaginal size, color pattern and slight differences in shape of genital structures. While I consider *S. occidentalis* a subjective junior synonym of *S. bouyeri* for this study, I do not establish synonymy formally as it would require careful examination of the primary types of both *S. occidentalis* and *S. bouyeri*, as well as a detailed assessment of the variation found in populations.

All aforementioned records of *Sinobirma* are from mid-altitude regions (ca. 1000–2500 m) in humid subtropical northern Burma, southwestern China and northeastern India, mainly for May–June. Therefore, all three species are likely univoltine summer flyers in the southeastern Himalayas. Apart from Burma, the genus has not been reported from any other areas of the Indochinese Peninsula. Chandra et al. (2019: 206) included Thailand in the distribution of *S. bouyeri* without any supporting data and specimen, which is why it is here regarded as an erroneous record.

To learn more about the biology and evolutionary history of the genus *Sinobirma*, this study explores and documents the complete life-cycle of a representative species, *S. bouyeri*, for the first time. This includes tests

of dozens of putative host plants, and the discovery of the first parasitoid. Furthermore, this study aims to test evolutionary and biogeographic hypotheses proposed in earlier literature (Nässig and Oberprieler 1994; Rougerie et al. preprint) by reconstructing phylogenetic relationships among *Sinobirma* and several Old World saturniid tribes based on mitogenomics.

2. Materials and methods

General equipment and usage: Vernier caliper INSIZE 1108-150C 0–150 mm / 0.01 mm (± 0.02 mm) and measuring microscope PEAK 2008-50X 0–1.6 mm / 0.02 mm were used to measure general lengths of immature material and to calibrated scale bars shown in figures. Balance XINGYUN FA1204E 120 g / 0.0001 g (± 0.0002 g) was used to determine the mass of pupae. Illuminometer BENETECH GM1020 (≤ 10000 Lux ± 3%; ≥ 10000 Lux ± 4%) was used for recording illuminance in the study of larval circadian rhythm. Fluorescent tubes PHILIPS TL 6W (UV-A, peak: 365 nm), QIANPU UVB-313EL 6W (UV-B, peak: 313 nm) and PHILIPS TUV 6W (UV-C, peak: 254 nm) were used for fluorescence tests and photographs of mature larvae. Soil pH, humidity and temperature were recorded by a data logger SMART SENSOR PH328 (± 0.2 pH; ± 4 RH%; ± 1.5°C), while hygrothermograph BENETECH GM1365 (± 2 RH%; ± 0.3°C) was used for recording of relative humidity and temperature during rearing. All color figures were photographed with a NIKON D5500 DSLR with SIGMA 10–20 mm f/4–5.6 lens or LAOWA 60 mm f/2.8–22 lens. Scanning electron microscope [SEM] images were taken with a ZEISS GeminiSEM 360. SEM samples of *S. bouyeri* were surface-dried and sputter-coated: Two unhatched ova, two larval head capsules of each L_1 and L_5, and one whole L_1 larva. Scoli and their distribution map in Fig. 2 were hand-drawn with pens of the COPIC Multiliner series.

2.1. Basic samples and rearing

In 2020, I received papered females of *S. bouyeri* from southeastern Tibet. One ♀ had been collected at the type-locality Bomê County, 2111 m, on 23 June, and 2 ♀♀ had been collected in Nyingchi City, 2052 m, on 22 June. From all of these, only one egg was obtained, off-white in color and not hatching during that year. I opened it on 05 April 2021; there was no embryo inside. During my expedition to the southern border of Tibet in the summer of 2021, 2 ♂♂ and 1 ♀ of *S. bouyeri* were captured during the nights of 26–29 June, at 2134 m in Mêdog County. Unfortunately, this female also laid only a single ovum in the paper triangle envelope, and it was lost on the following ecological survey. On 17 June 2022, I went back to the place, 12 ♀♀ and 3 ♂♂ were collected during the next 10 days. The females finally oviposited in a closed cylindrical net-cage (1.8–2.2 mm mesh), which was hung outdoors away from the vegetation in Mêdog. These caged eggs were later collected into a gauze bag (single mesh opening width: ca. 0.1 mm) and driven back to the research site in Kunming City, Yunnan, at an elevation of 1940 m. The eggs were placed indoors in a gauze cage (0.3 mm mesh) on a piece of mesh suspended ca. 1 cm above a moisture-saturated cotton pad, and sprayed with water every day. The resulting air humidity surrounding the eggs was ca. 80–95% RH at a temperature of ca. 17–21°C.

Newly hatched caterpillars were offered a large variety of host plants. A total of 35 species within 26 families of plants were chosen for the tests to larvae (sections 3.2.1–3.2.26), including 11 families commonly fed by African saturniids, and several families used to breed Asian species in the subfamilies Saturniinae, Salassinae and Agliinae. Also plants from a few other families found in the natural habitat of *S. bouyeri* were offered. All plants were collected in northern Kunming at elevations of ca. 1800–2000 m, using only fresh stems and leaves without pesticide contamination. Newly hatched larvae were offered plants the same day and sealed with just one plant species each in a plastic zip lock bag for observation. Feeding behaviour was recorded after 24 hours, and larvae that rejected their plant were switched to another plant species for testing. If feeding was confirmed, the lower parts of the plant's stems were inserted into a bottle filled with water (gaps in the bottleneck were closed with tissue paper). Plants with larvae were placed in a separate cage to continue observations indoors or outdoors.

After feeding had ended (after the liquid defecation), larvae were placed in a container with 9–10 cm of loose and uniform peat soil at the bottom for pupation (peat had been produced naturally from Heilongjiang Province of China; ca. 0.35–0.47 g/cm³ with moisture and holes, pH 6.28–6.51, 20.8–24.3°C and 52.6–61.4% RH). The soil surface was covered with ca. 1–2 cm of *Sphagnum* moss (Sphagnaceae) and several fallen walnut leaves.

2.2. Mitochondrial DNA sequencing and phylogenetic analyses

This work supplements here a circular sequence of the complete mitochondrial genome of *S. bouyeri* [GenBank: OR754233], its specimen data and high-throughput files have been uploaded to NCBI [BioProject: PRJNA905660].

DNA sequence data were generated from a fresh L_4 caterpillar of *S. bouyeri* [BioSample: SAMN31802199], which was killed and preserved in 95% (± 5%) ethanol at –18°C. DNA was extracted with chloroform-isoamyl alcohol and fragmented by ultrasonication. DNA library preparation (Illumina DNA Prep #1000000025416) included end repairing, 3'-end adenylation and ligation of sequencing adapter. Size selection was carried out on an agarose gel prior to amplification by PCR. After clean up and check, qualified libraries were sequenced on an ILLUMINA NovaSeq 6000. The resulting data [SRA: SRR22414765] were de novo assembled with SPAdes

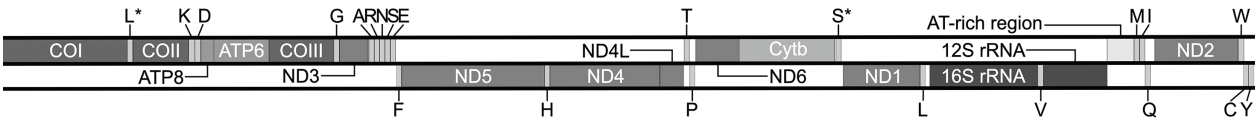

Figure 1. Linear map of the complete mitochondrial genome of *Sinobirma bouyeri* [OR754233].

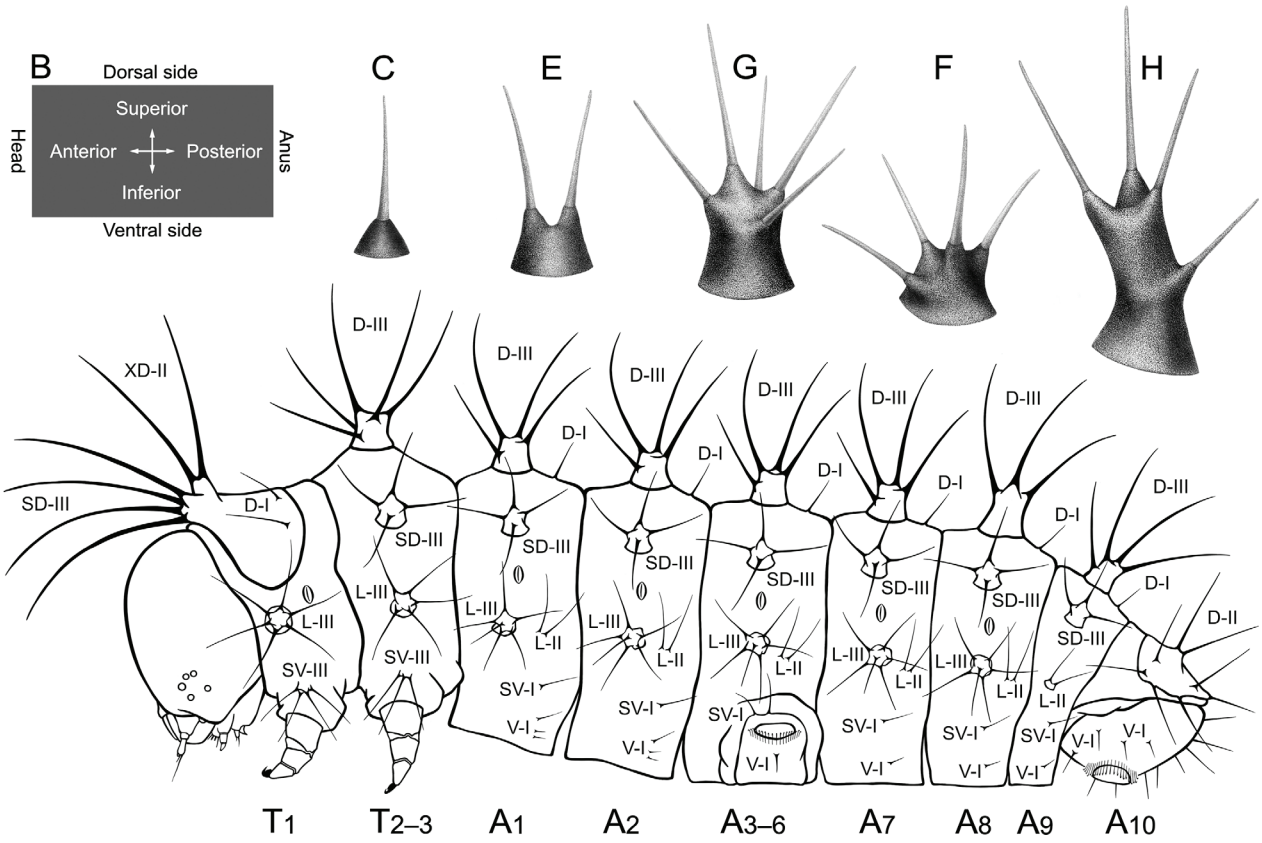

Figure 2. T_1–A_{10} Chaetotaxy [primary setae] of *Sinobirma bouyeri* L_1 in lateral view, not shown the setae of head capsule and legs $T_{1–3}$, and proleg A_{10} displays the medial surface, the ventral midline constitutes the bottom margins of $A_{1–9}$; **B** guidelines, the gray rectangle represents "lateral"; **C**, **E**–**H** Warts of *Sinobirma bouyeri* L_5; **C** chalaza (e.g., V-I, SV-I, D-I); **E** bifurcated scolus with a small (e.g., L-II, D-II) or medium-sized base (e.g., XD-II); **F** asterisk-like scolus with a small base (e.g., SV-III); **G** asterisk-like scolus with a medium-sized base (e.g., L-III, SD-III); **H** asterisk-like scolus with a large base (e.g., D-III).

3.15.4 (Prjibelski et al. 2020) using default parameters. The assembled mitochondrial genome had a length of 15,281 bp and was annotated using MITOS2 (Donath et al. 2019). Annotations were visualised as a mitochondrial genome map with OGDRAW (Greiner et al. 2019) and re-drawn as a linear plot in PHOTOSHOP BETA 25.0 (Fig. 1).

Phylogenetic trees (Fig. 15) were estimated from all codon positions of the 13 protein-coding mitochondrial genes [PCGs], namely COI, COII, ATP8, ATP6, COIII, ND3, ND5, ND4, ND4L, ND6, Cytb, ND1 and ND2. These PCGs were extracted from the complete mitochondrial genome of *S. bouyeri* and an additional 17 species with publicly available data (Jiang et al. 2009; Chen et al. 2014; Langley et al. 2020; Nethavhani et al. 2022; Kim et al. 2022). These additional sequences were from Asian-African Saturniidae, and Bombycidae as an outgroup (Table S6).

MAFFT V7 (Katoh et al. 2019) was used with default parameters to align the sequences. Maximum likelihood (ML) analyses with 1,000 bootstrap replicates were carried out in MEGA X (Kumar et al. 2018) using the recommended model GTR + G + I model, and ML analyses with 10,000 ultrafast bootstrap replicates (Hoang et al. 2018) in IQ-TREE 1.6.12 (Nguyen et al. 2015) using the best-fit model GTR + F + R3 (Kalyaanamoorthy et al. 2017). The IQ-TREE result (Fig. 15) was prepared in AFFINITY PHOTO 1.10.5.

2.3. Terminology and chaetotaxy

Homology of morphological structures, chaetotaxal terminology and its abbreviations follow Liu (2023): $L_{1–6}$ = 1st–6th larval instars; $T_{1–3}$ = 1st–3rd thoracic segments; $A_{1–10}$ = 1st–10th abdominal segments; O = ocellar; SO = subocellar; F = frontal; AF = adfrontal; C = clypeal; G = genal; A = anterior; V = ventral; SV = subventral; L = lateral; M = medial; D = dorsal; SD = subdorsal; XD = tactile dorsal; MD = microdorsal; P = parietal; S = stem-

ma; BaS = sensillum basiconicum; ChS = sensillum chaeticum; TrS = sensillum trichodeum; PlS = sensillum placodeum; CaS = sensillum campaniformium; DiS = sensillum digitiformium; StS = sensillum styloconicum; SP = sensory pore; -I: uni-setal, 1 seta; -II = bi-setal type, 2 setae; -III = multi-setal, more than 2 setae.

3. Results

The information provided in this section is based specifically on the *S. bouyeri* as a representative of the genus *Sinobirma*.

3.1. Morphology of preimaginal stages

In the sections 3.1.1–3.1.7, the lengths, widths, heights, and quantitative statistics (e.g., the quantity of setae and crochets) are based on single individual observations, unless otherwise specified. The widths of head capsules (for each sample, it is the distance between the pair of S6) are derived from the optimal host plant from the tests (see section 4.2).

3.1.1. Ovum (Figs 3, 11F, G)

Elongated sphere (length 1.71 mm, width 1.16–1.21 mm; n = 8); the micropylar area is located on the slightly more flattened short end (Fig. 3A–C). The exochorion has an off-white color and carries shallow, reticulated crests [chorionic sculptures] of approximately ca. 3 µm height and ca. 5 µm width (Fig. 3D), giving the appearance of a polygonal network. The aeropyles are approximately oval in shape, without crowns (Fig. 3E–F) and located at the junctions of the reticular crests. Most of them are ca. 3–5.5 µm in width, but a few are distinctly smaller (ca. 0.5–1.2 µm). The micropylar rosette is a sub-rounded region with an external diameter of ca. 150 µm (Fig. 3G). Each of its fragments is a slightly bulging polygon, while the outer part of the rosette is a relatively flat buffer zone (reticulated crests reduced) with a width of ca. 50 µm. In one sample I observed a foreign matter (possibly derived from the ovariole), ribbon-shaped, of ca. 38 µm length and attached to the center of the micropylar area (Fig. 3G). The surface of all eggs is unevenly covered by dark brown glue secreted from the female's accessory glands [colleterial glands].

3.1.2. L_1 (Figs $2T_1$–A_{10}, 4, 5, 7A, B, 12A–D)

Head capsule. Cervacoria is translucent dark gray; the width of the shiny black head capsule is 837.2 µm, with a dark grey anteclypeus; the 17 longer primary setae are borne on the head capsule, i.e., P1, P2, L1, AF1, AF2, F1, C1, C2, A1, A2, A3, O1, O2, O3, SO1, SO2 and SO3 (Fig. 4A, E). Except for the setal pairs of F1, SO1, SO2 and SO3, which have relatively smooth surfaces, all other setae have scaly surfaces (e.g., Fig. 5J). Within the group, seta P1 is always the longest, with a length of 540.3 µm. Setae F1 and SO1 usually appear to be the shortest, the former having a length of 91.6 µm and the latter of 98.2 µm. Observation of a random selection of five setae (F1, C2, AF1, L1 and A3) in a single specimen revealed these to be hollow. Furthermore, four pairs of minute primary setae MD1, MD2, MD3 (Figs 4A, E, 5A, B) and G1 (Fig. 4E) are present on the head capsule, each with a smooth surface. In this group, setae MD2 and MD3 are the lon-

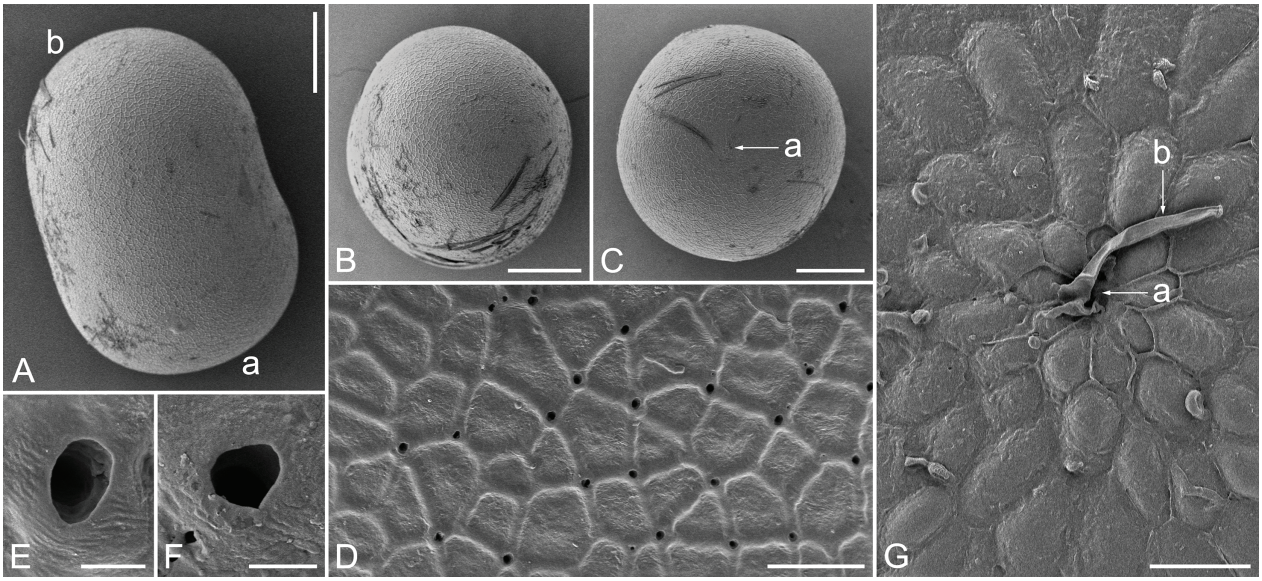

Figure 3. Ova of *Sinobirma bouyeri*. **A** Lateral view, scale bar = 400 µm; a: micropylar side; b: non-micropylar side. **B** Non-micropylar side, vertical view, scale bar = 350 µm. **C** Micropylar side, vertical view, scale bar = 350 µm; a: micropylar zone. **D** A part of exochorion in the non-micropylar area, scale bar = 40 µm. **E** Aeropyle, scale bar = 4 µm. **F** Aeropyle, scale bar = 3 µm. **G** Micropylar zone, scale bar = 20 µm; a: central area; b: foreign matter.

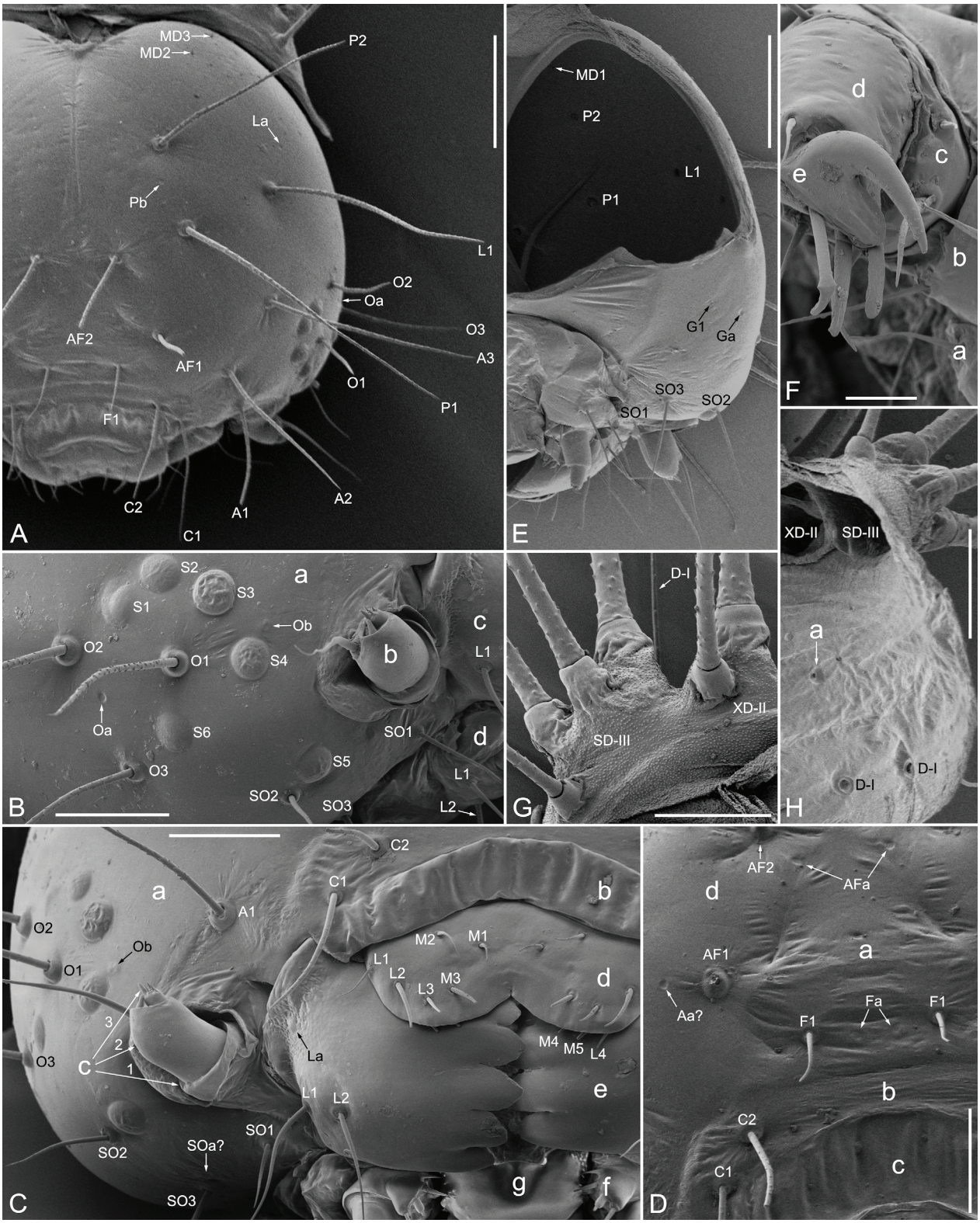

Figure 4. L_1 of *Sinobirma bouyeri*. **A**–**E** Cephalic regions. **A** Frontal view, scale bar = 200 μm. **B** Lateral view, scale bar = 100 μm; a: head capsule; b: antenna; c: mandible; d: maxilla-hypopharynx-labial complex. **C** Frontal view, scale bar = 100 μm; a: head capsule; b: anteclypeus (a part of the head capsule); $c_{1–3}$: the 1st–3rd antennal segments; d: labrum; e: mandible; f: maxilla; g: hypopharynx. **D** Frontal view, scale bar = 100 μm; a: frons; b: clypeus; a + b: frontoclypeus; c: anteclypeus; d: other area of the head capsule. **E** Posterior view, scale bar = 200 μm. **F** Leg T_3, apical view, scale bar = 40 μm; a: coxa; b: femur; c: tibia; d: tarsus; e: pretarsus. **G** Prothoracic shield, frontal view, scale bar = 100 μm. **H** Prothoracic shield, ventral view [the inner surface], scale bar = 100 μm; a: secondary seta.

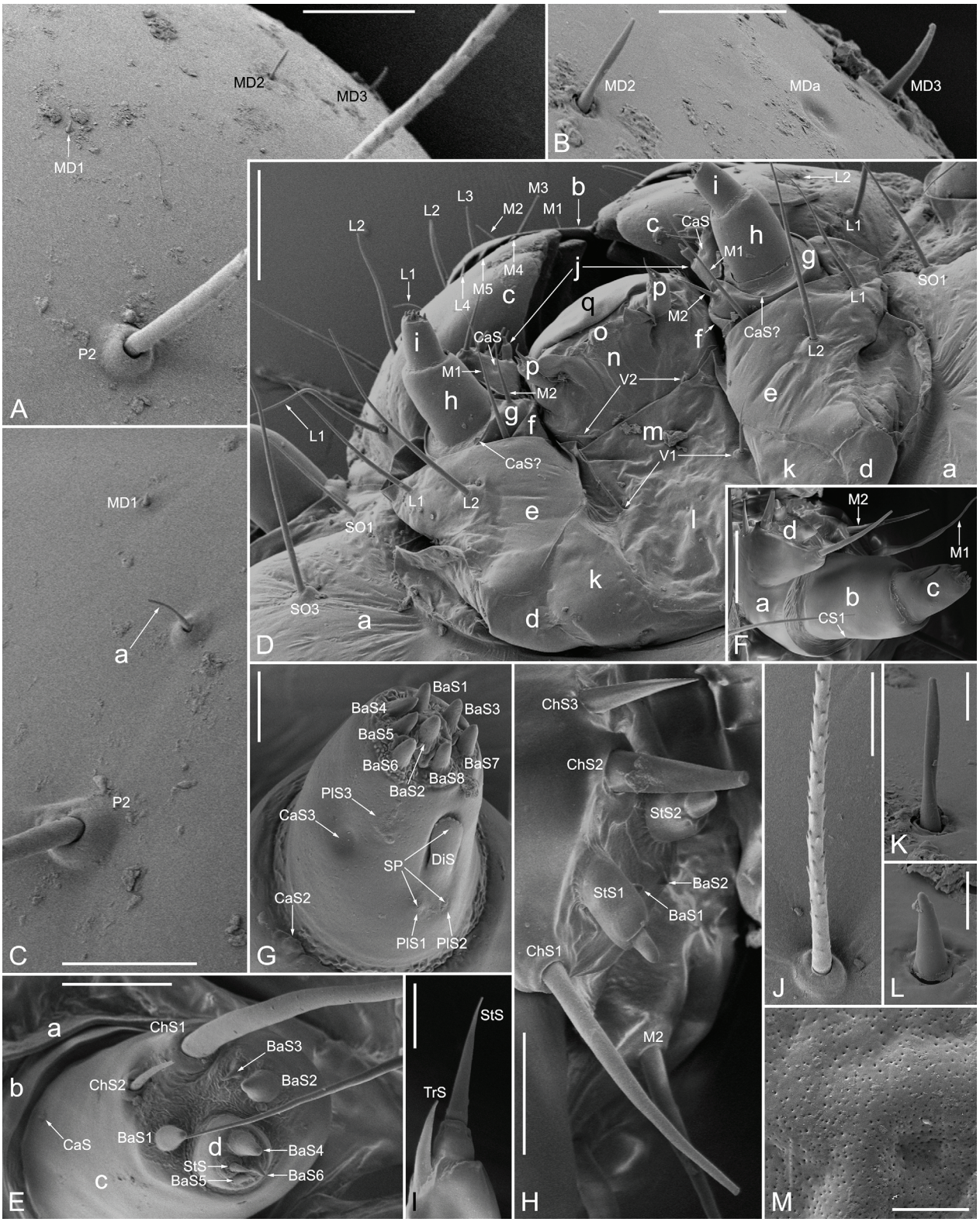

Figure 5. L_1 of *Sinobirma bouyeri*. **A**–**M** Cephalic regions. **A** Head capsule, frontal view, scale bar = 50 µm. **B** Head capsule, frontal view, scale bar = 20 µm. **C** Head capsule, frontal view, scale bar = 50 µm. **D** Posterior view, scale bar = 80 µm; a: head capsule; b: labrum; c: mandibles; d–j: maxillae; d: cardines; e: stipites; f: palpifers; g–i: the 1st–3rd maxillary palpal segments; j: maxillary mesal lobes; k–q: labium; k: submentales l: postmentum; m: mentum; n: prementum (posterior); o: spinneret; p: labial palpi; q: prementum (anterior). **E** Lateroapical view, scale bar = 30 µm; a: antacoria; b–d: the 1st–3rd antennal segments. **F** Dorsal view, scale bar = 40 µm; a–c: the 1st–3rd maxillary palpal segments; d: maxillary mesal lobe. **G** The 2nd–3rd maxillary palpal segments, dorsoapical view, scale bar = 10 µm. **H** The distal area of maxillary mesal lobe, dorsal view, scale bar = 20 µm. **I** The distal area of labial palpus, ventral view, scale bar = 10 µm. **J** Seta P1, scale bar = 50 µm. **K** Seta MD2, scale bar = 5 µm. **L** Seta MD1, scale bar = 4 µm. **M** Part of the external surface [epicuticle] of S3, scale bar = 4 µm.

Table 1. *Sinobirma bouyeri* L_1, a quantity statistic of chalazae/scoli (outside brackets) on the single side (divided along the dorsal and ventral midlines), with the numbers of primary setae (inside brackets) borne on each of them. See also Fig. 2.

Structures\Segments	T_1	$T_{2–3}$	A_1	A_2	$A_{3–6}$	A_7	A_8	A_9	A_{10}
Scoli D-III		1(5)	1(4)	1(4)	1(4)	1(4)	1(3)	1(4)	
Scolus D-II									1(2)
Chalazae D-I	2(1)		1(1)	1(1)	1(1)	1(1)	1(1)	1(1)	
Scolus XD-II	1(2)								
Scoli SD-III	1(4)	1(4)	1(4)	1(4)	1(4)	1(4)	1(4)	1(3)	
Scoli L-III	1(6–7)	1(5)	1(6)	1(6–7)	1(6)	1(6)	1(6)		
Scoli L-II			1(2)	1(2)	1(2)	1(2)	1(2)	1(2)	
Scoli SV-III	1(4)	1(3)							
Chalazae SV-I			1(1)	1(1)	2(1)	1–2(1)	1(1)	1(1)	
Chalazae V-I			3(1)	3(1)	1(1)	1(1)	1(1)	1(1)	4(1)

gest at ca. 16 μm and erect, but sometimes slightly twisted (e.g., Fig. 5K); seta MD1 is a sensillum basiconicum and the shortest at 6.1 μm (Fig. 5L). In one case, a specimen had a secondary seta on only one side (asymmetry) of the head capsule, located between setae MD1 and P2 (Fig. 5C). The six pairs of stemmata have a similar diameter of 36–41 μm (Fig. 4B) and are densely covered with microscopic pores (e.g., Fig. 5M); S1 is the flattest one, and S3 is the most protruding. The head capsule carries eight distinctive pairs of primary pores, most of which appear as a pit with a flat bottom: Pb, La, AFa, Fa, Oa, Ob, MDa, and Ga (Figs 4A–E, 5B). Pore Ob is morphologically unique, appearing as a somewhat elevated annulus (Fig. 4B, C). There are multiple irregularly shaped pits in the subocellar area, making the accurate observation of pore SOa difficult (Fig. 4C); a primary pore laterally of seta AF1 is potentially pore Aa? [Pa?] (Fig. 4D).

Antenna. The 2nd segment of the antenna has the largest exposed areas (Figs 4C, 5E), colored a smooth rust red and bearing a very strong ChS1 (224.4 μm length) at its apical end, with ChS2, BaS1, BaS2 and BaS3 smaller in size, whereas CaS is more proximal on the lateral surface, near the 1st antennal segment. The 3rd antennal segment is minute, with BaS4, BaS5 and BaS6 located at its apex; it also carries a StS, which has an elevated base forming a sclerotized annulus. BaS1, BaS2 and BaS4 are similarly shaped with a rounded apex and relatively larger than BaS3, BaS5 and BaS6, which have more pointed tips.

Mouthparts. Primary setae L1, L2, L3, M1, M2 and M3 (Figs 4C, 5D) are situated on the anterior surface of the labrum, while setae L4, M4 and M5 are present on the posterior surface [epipharynx]. Ventrally of the labrum, each mandible carries two strong primary setae L1 and L2, with a primary pore La (Figs 4C, 5D). The maxillary palpus is 3-segmented, with its 1st segment corresponding to the mesal lobe [galea] (Fig. 5F); the cardo is smooth; the stipes carries two primary setae L1 and L2 (Fig. 5D); the palpifer bears primary seta M1 near its apex and close to the 1st palpal segment, which carries apically the primary seta M2 and ventroapically a slight bulge [CaS?]. The 2nd maxillary palpal segment carries CaS1 and CaS2, which appear as a flat-bottomed pit and a minute latero-distal wart, respectively (Fig. 5F, G). PlS1, PlS2 and DiS are located on the dorsal area of the 3rd maxillary palpal segment (Fig. 5G); the former two are elevated slightly with granulated surfaces, located at the proximal area of DiS, each of them has a central SP. DiS has a terminal serrated margin, with the SP clearly visible in its flat part. On the same segment, CaS3 is a large dorsolateral smooth pit, with an inconspicuous rough PlS3 near it. There is a group containing 8 erect sensilla attached to the rugose terminal area of the segment, similar in shape and size to each other. Among them, BaS1, BaS2 and BaS3 are multiporous with rounded tips, whereas BaS4, BaS5, BaS6, BaS7 and BaS8 are smoother with papilliform apices. The apex of each maxillary mesal lobe bears 7 conspicuous sensilla, labeled as ChS1, ChS2, ChS3, StS1, StS2, BaS1 and BaS2 (Fig. 5H). The longest ChS1 is 48.5 μm in length, located in the most lateral position. In some specimens, ChS1 and ChS2 are flat-topped, but it is uncertain if these are damaged or if this is their natural shape. Each of StS1 and StS2 has a longitudinally plicated annulus attached to its basal area. BaS1 and BaS2 are small, and while the former nears the center of the distal surface adjacent to StS1, BaS2 arises next to StS2 and close to the ventroapical margin. On the ventral area of the mesal lobe, a CaS is located subapically (Fig. 5D). Finally, paired postmental [submental] setae V1 and premental [stipular] setae V2 are also placed in the setal group of the whole maxilla-hypopharynx-labial complex (Fig. 5D). The spinneret resembles a cleft extending transversally between the labial palpi (Fig. 5D). Each labial palpus terminates with a lateral TrS and a medial StS (Fig. 5I). No hypopharyngeal microstructures were observed.

Thorax and abdomen. The chaetotaxy is as illustrated (Fig. $2T_1$–A_{10}) and counted (Table 1). On each side (divided along the dorsal and ventral midlines), there are two setae located on the posterior side to scolus L-III on each of $A_{1–8}$, in the same larval specimen, they are borne on a unitive black base or separated away from each other, but here all named as scolus L-II. Basal parts of scoli D-III of A_8 are medially fused, forming the largest wart of the whole body. On each side of the prothoracic shield, there are two slightly elevated and minute tubercles namely chalazae D-I, however, secondary hair sometimes

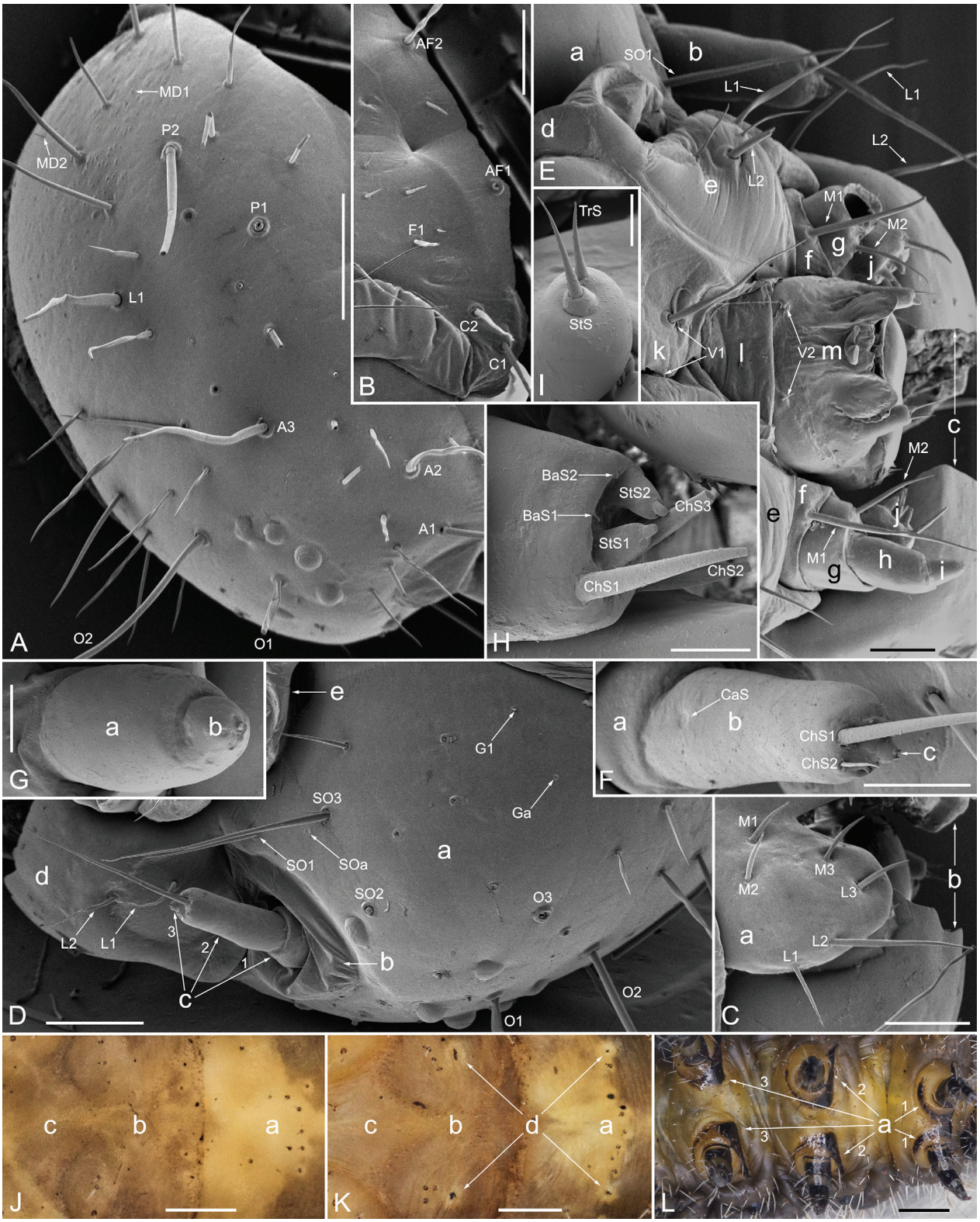

Figure 6. L_5 of *Sinobirma bouyeri*. **A** Head capsule, frontal view, scale bar = 800 µm. **B** Head capsule, frontal view, scale bar = 500 µm. **C** Frontal view, scale bar = 300 µm; a: labrum; b: mandibles. **D** Posterolateral view, scale bar = 500 µm; a: head capsule; b: antacoria; $c_{1–3}$: the 1st–3rd antennal segments; d: mandible; e: maxilla-hypopharynx-labial complex. **E** Posterior view, scale bar = 200 µm; a: head capsule; b: antenna; c: mandibles; d–j: maxillae; d: cardo; e: stipites; f: palpifers; g–i: the 1st–3rd maxillary palpal segments; j: maxillary mesal lobes; k–m: labium; k: postmentum; l: mentum; m: prementum (posterior). **F** Lateroapical view, scale bar = 200 µm; a–c: the 1st–3rd antennal segments. **G** Ventroapical view, scale bar = 80 µm; a–b: the 2nd–3rd maxillary palpal segments. **H** Maxillary mesal lobe, ventral view, scale bar = 60 µm. **I** labial palpus, medioapical view, scale bar = 40 µm. **J** ♂, ventral view, scale bar = 1 mm; a–c: $A_{8–10}$. **K** ♀, ventral view, scale bar = 1 mm; a–c: $A_{8–10}$; d: sexual gland. **L** Ventral view, scale bar = 2 mm; a1–3: coxal sclerites $T_{1–3}$.

appears (e.g., Fig. 4H). The proximal parts of contiguous scolus XD-II and scolus SD-III are medially fused on the anterior margin of prothoracic shield (Fig. 4G, H); their setae are translucent pale brown, curved and longer than that of any other scoli; setae of scoli D-III similarly colored. All scoli have black or gray bases, those of the prominent scoli D-III very smooth and shiny. The ground color of T_1–A_{10} is light yellow, both anterior and posterior sides of each scoli SD-III on T_2–A_9 are marked with dark gray spots irregular in shape and size. Spiracles are brown and located within a dark gray spot. The prothoracic shield is very large (ca. 800 μm × 330 μm) and shiny black, as are the lateral plates of prolegs A_{10} and the sclerotized parts of legs $T_{1–3}$, except for the pretarsi that are dark maroon in color. Basal sclerites of coxae are shaped incomplete annular, and only the pair on T_1 are medially fused. Six primary setae arise from each coxal sclerite: the longest and the shortest one side by side and close to the anterolateral apex, three setae on the medial arc, and one seta arising at the posterolateral apex. Each femur bears a pair of apical setae on the medial area. The tibia has two lateroapical setae and four medioapical setae. The tarsus ends with four setae, three of which are medial and broadly flattened, the other one being pointed and located laterally. Each pretarsus shows a very well developed basal lobe (Fig. 4F). The prolegs and plantae of $A_{3–6}$ and A_{10} are vivid yellow with dark brown crochets (19–22 in number) in uniserial heteroideous mesoseries. In most specimens, the anterior and posterior sides of each scolus D-III on $A_{1–7}$ are marked with light gray spots, but in other individuals these spots are indistinct to not apparent. The dorsal midline is conspicuous and light gray on $A_{1–9}$. The anal shield is a black, shiny triangle; in dorsal view, the posterior margins of the pair of lateral plates of the prolegs A_{10} join to form a minor arc outline.

3.1.3. L_2 (Figs 7C, D, 12D–F)

The width of head capsule increases to 1.31 mm. Many secondary setae are visible on the integument, especially the ventral area. In dorsal view, T_1–A_{10} are black in color, with discontinuous pale yellow middorsal stripes on T_1–A_8. The bases of scoli D-III are still prominent and are the largest; scoli D-III, XD-II and SD-III have shiny red bases and bear reddish orange spiny setae, with the setae of scoli XD-II and SD-III of T_1 the longest. Chalazae SV-I, scoli L-II and L-III have ochre bases, while scoli SV-III and chalazae V-I have gray bases. The ventral area of $T_{1–3}$ is dark gray, but it is yellowish for $A_{1–10}$. For each of the legs $T_{1–3}$, the pretarsus and tarsus are dark maroon, the tibia and femur shiny black, and the coxa gray. The posterolateral margins of prolegs A_{10} are ocher around their lateral plates. Pale yellow stripes, discontinuous and nearly crescent-shaped, are visible between the scoli D-III and SD-III on $A_{1–8}$, and likewise some irregularly shaped stripes of the same color around the black spiracles of these segments. In lateral view, the dorsal junction area between A_1/A_2 is the most sunken area, conspicuous when a larva rests on a plant. Prolegs, plantae and crochets of $A_{3–6}$ and A_{10} are identical in color as in L_1, but the plantae are wider and bear uniserial homoideous mesoseries of 24–26 crochets.

3.1.4. L_3 (Figs 7E, F, 12G)

Head capsule is 2.17 mm in width. The prothoracic shield starts to split along the dorsal midline, in some individuals this "fissure" appeared as multiple irregular and discontinuous depressions. The ventral areas of most segments are gray, but fade to yellow on $A_{7–9}$. A larger number of minute, white secondary setae are visible in the dorsal area, especially around D-III — a scolus significantly more elevated than in the L_2 and with its inferior basal parts turning into a smooth black, but the superior area shiny red. Each scolus D-III bears strong brown spines, but the longest setae are still those on scoli XD-II and SD-III of T_1. Except for those in the middorsal area, the yellow stripes described in L_2 are vivid lime green, especially in the lateral areas of T_1 and $A_{1–8}$. All proleg bases and plantae look more developed and inflated than in L_2. All prolegs have a goldenrod ground color, and each of them exhibits 42–45 reddish brown crochets in biordinal mesoseries. The posterior tip of the shiny black anal shield is more elongate than in L_2.

3.1.5. L_4 (Figs 7G, H, 12H)

Head capsule width is 3.24 mm; the shiny black prothoracic shield has a fissure along the dorsal midline, but it isn't fully split yet. All the bases of scoli are shiny black, most of them with translucent brown spiny setae, but the strongest and longest setae of scoli D-III have turned into almost opaque black. The bases of scoli XD-II and SD-III on T_1 are significantly more elevated than in L_3. Ground color of the whole ventral area is brownish gray, and T_1–A_{10} bear more white secondary setae on the lateral areas of the integument. There are several lime green "Y-shaped" strips ornamenting the dorsal midline of T_2–A_8. The lateral stripes that appeared in L_2 are wider and developed into lime green patches, the largest ones of which have black dots in their centers on $A_{1–8}$. On each side of $A_{1–7}$, an ochre strip connects scolus D-III, scolus SD-III and the spiracle. The lateral plates of prolegs $A_{3–6}$ and A_{10} are black and smooth; their plantae are vivid yellow, each bearing 50–55 maroon crochets arranged in biordinal mesoseries. The posterior margin of the anal shield is elongated into a short spine, more pronounced than in L_3.

3.1.6. L_5 (Figs 2C, E–H, 6, 7I–O, 9B, 12I, 14A–D, 15)

This is the final larval instar under normal conditions (but see section 3.2.10 for a case of L_6). The head capsule is 4.74 mm in width. Its epicranial suture, ecdysial lines, anteclypeus and the antacoriae are off-white. The medial margin of the labrum is bronze color, the frontoclypeus a dark brown with a pair of triangular black spots in its center (Fig. 7O). The distribution of the 17 pairs of long primary setae is similar to L_1, i.e., of P1, P2, L1, AF1, AF2, F1, C1, C2, A1, A2, A3, O1, O2, O3, SO1, SO2 and SO3 (Fig. 6A, B, D). That is also the case for four pairs

Figure 7. Larvae of *Sinobirma bouyeri*. **A**, **G**–**O** Reared on *Coriaria nepalensis*; **B**, **D**–**F** Reared on *Prunus cerasoides*; **C** Reared on *Salix babylonica*. **A** L_1, lateral view, scale bar = 1 mm. **B** L_1, dorsal view, scale bar = 1 mm. **C** L_2, lateral view, scale bar = 2 mm. **D** L_2, dorsal view, scale bar = 2 mm. **E** L_3, lateral view, scale bar = 3 mm. **F** L_3, dorsal view, scale bar = 3 mm. **G** L_4, lateral view, scale bar = 5 mm. **H** L_4, dorsal view, scale bar = 5 mm. **I** Freshly moulted L_5, lateral view, scale bar = 5 mm. **J** L_5, lateral view, scale bar = 7 mm. **K** L_5, dorsal view, scale bar = 7 mm. **L** L_5, ventral view, scale bar = 7 mm. **M** Planta A_4 of L_5, ventrolateral view, scale bar = 1 mm. **N** $A_{8–10}$ of L_5, lateral view, scale bar = 3 mm. **O** Cephalic regions and $T_{1–2}$ of L_5, anterolateral view, scale bar = 2 mm.

of minute setae MD1, MD2, MD3 and G1. In addition, many secondary setae are present on the head capsule. All the cephalic setae have smooth surfaces, some slightly helical in shape. Some broken setae reveal their hollowness, as in L_1 (e.g., Fig. 6A). Primary pores could not be observed, but Ga and SOa are clearly present (Fig. 6D).

The conspicuous sensilla located on the 2nd and 3rd antennal segments in L_1 are significantly reduced in size in L_5; only ChS1, ChS2 and CaS are still strongly developed (Fig. 6F). The sensilla of the 3rd segment of the maxillary palpus are less pronounced (Fig. 6G), but ChS1, ChS2, ChS3, StS1, StS2, BaS1 and BaS2 of the maxillary mesal lobe are still very distinct (Fig. 6H). The general shape of the labium (e.g., the spinneret and TrS, StS of the labial palpi) is similar during $L_{1–5}$ (Fig. 6E, I). The primary setae borne on the labrum (L1, L2, L3, M1, M2, M3, L4, M4 and M5; e.g., Fig. 6C), on the mandibles (L1 and L2) and on other areas of maxilla-hypopharynx-labial complex (L1, L2, M1, M2, V1 and V2) are still conspicuous and strong (Fig. 6E), although several secondary setae appeared on the surface of the latter structure in L_5.

Compared to L_4, the general habitus of L_5 is nearly identical, with a cylindrically shaped larva that has the largest volume in A_3 and A_4. The most obvious difference to L_4 is that the lime green middorsal strips are wider, and that similar strips are now visible in the dorsal area of $A_{9–10}$. Many white secondary setae cover the larval integument; they are more numerous and visible than in previous instars, especially on the lateral and dorsal areas. The fusion of scoli D-III of A_8 is identical as in L_1.

In freshly molted specimens, most parts of the legs $T_{1–3}$ (except the dark maroon pretarsi), most parts of the prolegs $A_{3–6}$ (except the reddish maroon crochets), all chalazae/scoli, the head capsule and the whole A_{10} are bright goldenrod; these structures darken in fully hardened and tanned larvae (Fig. 7I). The color of hemolymph is also bright yellow. The ventral area is mostly dark brown to dark gray, but yellowish near the midline. It is noteworthy that when the caterpillar is fully grown and feeding ends, most parts of the ventral area turn into an amber color (e.g., Fig. 6J, K).

As in $L_{2–4}$, the dorsal area of the A_1/A_2 junction zone (sometimes together with T_3/A_1) can be observed as the most sunken area in lateral view. The shiny black prothoracic shield splits into two parts along the off-white middorsal fissure in L_5. The anal shield is large and triangular, its posterior tip distinctly elongated to form a strong spine as in L_4 (Fig. 7N). When resting, the posterior margins of the pair of lateral plates of the prolegs A_{10} usually combine into a minor arc outline in dorsal view, which is a characteristic that's similar in every instar since L_1 (not mentioned in sections 3.1.3–3.1.5). The 54–62 crochets borne next to the planta of each proleg $A_{3–6}$ and A_{10} are arranged to form biordinal mesoseries (e.g., Fig. 7M). The pair of coxal sclerites on T_1 present a similar fusion as described in L_1 (Fig. 6L). The sexual gland of female caterpillars ["Ishiwata's gland"] is conspicuous in the form of 4 lighter yellow dots on A_8 and A_9 (Fig. 6K). In contrast, the male sexual gland ["Herold's gland"] cannot be observed externally by eye (Fig. 6J).

3.1.7. Pupa (Figs 8, 14G, H)

The overall color of the epicuticle is black, but $A_{4–8}$ appear dark reddish brown. Female pupae are generally larger. The antennal margins are slightly elevated in males (Fig. 8C) and more flattened in females (Fig. 8E). The maxillae and legs $T_{1–2}$ are visible between the antennae in both genders, with the former long and wedge-shaped. All pupae bear two pairs of tubercles on the head (Fig. 8C–E). One lies in the central area on each side of the frontoclypeus midline, it is conical, minute, black and with a rough surface; the other pair is situated on each side of the labrum, it is semicircular, larger, black and with a smooth surface. All pupae also bear three pairs of dorsal tubercles (Fig. 8G) on the anterior margin of T_1 and the medial areas of $T_{2–3}$. The tubercles of T_3 are the largest, transversally elongated into semi-elliptical shapes, black and smooth, with many irregular small pits, which are sometimes fused into wrinkles. The tubercles of T_2 are smaller than those of T_3, shiny black, sub-circular in shape and with a wrinkly surface. The tubercles of T_1 have pointed fork-like tips, as each tubercle divides into two tips, of which the medial tip is further divided into two smaller tips. The thoracic spiracle, which is located at the center of the lateral area of T_1 during larval instars, is now located on the lateral area of the T_1/T_2 boundary, while the tracheal branch is still located inside T_1 and protected by an annular cap [external ring] over a cavity (Fig. 8G). The spiracles of $A_{2–8}$ have similar caps of elliptic shape over cavities (e.g., Fig. 8F). There are several annuli of slightly elevated crests on each of anterior areas (within the junction zones) of $A_{5–7}$, and each of the three segments has many short spines arranged uniserially, surrounding the anterior margins (Fig. 8F). A_8 has a single middorsal pointed tubercle of very small size, which is probably homologous with the larval scoli D-III. The cremaster on the tip of A_{10} is elongated into a very long and strong spine (Fig. 8H). Of the entire pupa, only the junction zones between A_4/A_5, A_5/A_6, and A_6/A_7 are less sclerotized flexible joints, all other joints are rigid. The male genital pore is located on the midventral area of A_9 (Fig. 8B), whereas the female pores are located along the ventral midline of A_8 [ostium bursae] and A_9 [ostium oviductus], respectively (Fig. 8D).

3.2. Host plant preference tests

Host plant preference was systematically tested by restricting batches of larvae to just one plant at a time, and observations are presented by plant family in the following sub-sections. To reduce the risk of larval infectious diseases for larvae indoors, the rearing density had to be reduced. Therefore, some of the larvae from plants discussed in sub-sections 3.2.4, 3.2.5, 3.2.10, 3.2.14, 3.2.22 and 3.2.24 were placed onto wild trees. This also provided an opportunity to collect potential parasitoids in the wild of Yunnan. However, all of these caterpillars were missing within a week, most probably preyed upon or having left the plants by themselves.

3.2.1. Sapindaceae

The larval group rejected *Sapindus saponaria*, but easily accepted *Acer buergerianum* after switching. Unfortunately, all of the ten individuals died together on the 4th day after feeding.

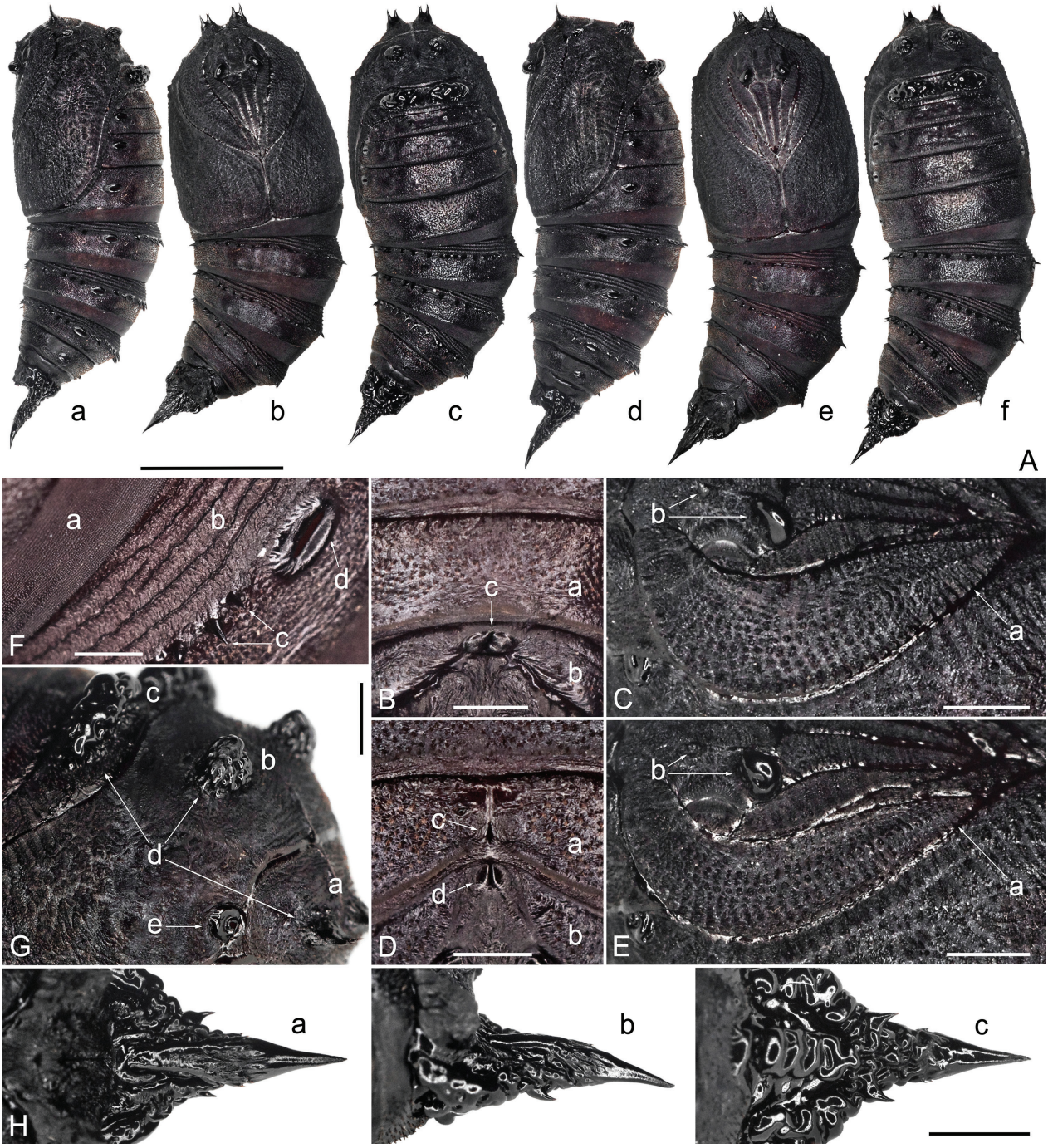

Figure 8. Pupae of *Sinobirma bouyeri*. **A** Scale bar = 10 mm; a: ♂, lateral view; b: ♂, ventral view; c: ♂, dorsal view; d: ♀, lateral view; e: ♀, ventral view; f: ♀, dorsal view. **B** ♂, ventral view, scale bar = 1 mm; a–b: $A_{8–9}$; c: genital pore. **C** ♂, ventrolateral view, scale bar = 2 mm; a: antenna; b: head tubercles. **D** ♀, ventral view, scale bar = 1 mm; a–b: $A_{8–9}$; c–d: genital pores. **E** ♀, ventrolateral view, scale bar = 2 mm; a: antenna; b: head tubercles. **F** ♀, lateral view, scale bar = 1 mm; a–b: $A_{4–5}$; c: abdominal tubercles; d: annular cap of spiracle. **G** ♀, anterolateral view, scale bar = 2 mm; a–c: $T_{1–3}$; d: thoracic tubercles; e: annular cap of spiracle T_1. **H** ♀, the long spiny cremaster on the tip of A_{10}, scale bar = 2 mm; a: ventral view; b: lateral view; c: dorsal view.

3.2.2. Fabaceae

None of the larvae (ten larvae each) accepted *Puhuaea* cf. *sequax* or *Albizia julibrissin*, but ten other larvae formed a cluster and quickly accepted *Robinia pseudoacacia*. These feeding larvae started to die after the 4th day, became restless (left the host plant) and finally all died before the first pre-molt, achieving a lifespan of only 4–8 days.

3.2.3. Anacardiaceae

Pistacia weinmanniifolia was quickly accepted by ten larvae, and these larvae increased visibly in size by the 3rd day. However, the following day most of the individuals moved restlessly and died the next day. The last larva died on the 7th day. A different batch of ten larvae performed similarly on *Pistacia chinensis*. Two batches of ten larvae each fed on *Rhus typhina* and *Toxicodendron*

vernicifluum, but began to die from the 3rd day. No larvae survived to L_2 on host plants of this family.

3.2.4. Salicaceae

The early development of 19 larvae on *Salix babylonica* was rapid during the first three days, but progress in growth started to vary significantly between individuals from the 6th day of L_1, because some individuals frequently left the larval cluster, causing inconsistency in their feeding behavior. All individuals molted from L_3 to L_4 on days 26th–31st, despite their variations in size; two larvae died of illness during L_3. The remaining 17 L_4 of this group died, either by sampling four specimens for morphological studies or when releasing them on a willow tree outdoors for further observations.

3.2.5. Fagaceae

Two groups of 10 larvae each were offered *Quercus yunnanensis* and *Quercus glaucoides*. As the leaves of the former were too hard, all individuals were switched to *Q. yunnanensis* on the 3rd day. These 20 larvae, which had all hatched on the same date, soon formed a single cluster and continued to feed. However, larval growth began to slow significantly from the 4th day, and a total of 6 individuals had died by the 7th day, while other larvae often crawled around restlessly. Consequently, oaks were judged to be unacceptable host plants in captivity. On the 7th day, before the first pre-molt, all of the remaining 14 individuals were taken to the same plant outdoors for continued observation.

3.2.6. Meliaceae

A group of 12 larvae was offered *Toona sinensis*. A minute gap in the edge of a leaf was observed on the 2nd day, but no further feeding occurred, and these larvae starved to death on the 4th day.

3.2.7. Ericaceae

The genus *Rhododendron* forms one of the most spectacular plant communities in the alpine ecosystem of the Himalayas. I encountered them in abundance as shrubs during my expeditions to Mêdog, at altitudes from about 1500 to 4100 m, distributed from humid subtropical forests to snow lines. However, *Rhododendron* cf. *pulchrum* was rejected by all ten larvae in my test.

3.2.8. Malvaceae

Similar to larvae on other host plants tested, a group of ten larvae quickly formed a tight cluster on a leaf of *Hibiscus syriacus*, but showed no sign of feeding on this plant.

3.2.9. Lauraceae

Only the evergreen plant *Cinnamomum camphora* was tested for this family, but rejected by all ten larvae.

3.2.10. Rosaceae

One of the first plants to be tested was *Prunus cerasoides*. Seventeen newly eclosed larvae easily accepted the plant, and an increase in size was observed for each specimen on the 3rd day. Larvae began to show differences in size starting with L_3, and burrowed in the soil as L_5. However, two larvae failed to pupate in the soil, while a single specimen molted to a weak L_6. The rearing of these larvae was documented in more detail (Table S1).

A further ten larvae were tested on *Pyrus pseudopashia* with similar result after three days, but since *P. pseudopashia* was scarce near the experimental site, the larvae were switched to *P. cerasoides* on the 4th day, which larvae quickly accepted and continued to grow. An additional 70 larvae that had rejected other plants were added, resulting in a total of 80 larvae of different ages feeding on *P. cerasoides*. As rearing progressed, only one larval molting failed from L_3 to L_4, and a further six specimens died of illness during $L_{2–4}$. The remaining larvae were released outdoors on *P. cerasoides* for further observation before entering L_5.

A group of 8 larvae were tested on *Rosa* cf. *multiflora*, but they began to die from the 5th day onwards (L_1). The last larva died as an early L_2, resulting in lifespans of only 5–12 days.

3.2.11. Magnoliaceae

During the field surveys in Mêdog and Bomê, *Magnolia* spp. were commonly encountered in the natural habitats of *S. bouyeri*. Therefore, *Magnolia denudata* was offered to ten larvae, but fully rejected.

3.2.12. Betulaceae

Alnus nepalensis appears to form dominant populations in the Sub-Himalayan valleys where I collected the adults of *S. bouyeri*, but the ten larvae offered this plant rejected it without any bite marks on the leaves.

3.2.13. Altingiaceae

Liquidambar formosana is one of the most commonly used host plants when rearing many Asian saturniids in captivity. A batch of ten larvae started to feed on this plant, while another seven larvae rejected it and clustered on the inner wall of the zip lock bag. Larvae that fed on the plant did not increase significantly in size during the first three days and died one by one before the first pre-molt, resulting in lifespans of 3–7 days.

3.2.14. Lythraceae

A total of ten larvae fed on *Lagerstroemia indica*, readily accepting the plant and growing faster than most others during the first 3 days. Therefore, an additional ten larvae that had rejected another plant were added. The hatching dates of the two larval batches differed by one day, but they soon formed a unified larval cluster. However, be-

cause some larvae aggregated at the mouth of the bottle, their feeding duration began to differ. The larvae eventually completed their first molt on the 8th–9th day after their respective hatching. Since L_2, growth rate of larvae slowed significantly, with size differences between individuals increasing. By the 19th day, all larvae were still in L_2 without pre-molt, making it the slowest batch to grow. Except for four larvae killed for morphological studies, the remaining 16 larvae were released on *L. indica* outdoors for continued observation.

3.2.15. Santalaceae

Osyris lanceolata is a common shrub in southeastern China, but all ten larvae rejected the plant.

3.2.16. Juglandaceae

Plants of this family are very useful for rearing a large number of saturniid species from around the world. Walnut tree is common in southern Tibet and western Yunnan. A batch of seven larvae fed on *Juglans regia* from hatching to first molting for 13 days, which is the longest of all comparable batches on other plants. Two larvae died on the 3rd day after entering L_2, and others died the following day.

3.2.17. Ulmaceae

A batch of ten larvae quickly accepted *Ulmus parvifolia* on the day of hatching, but all larvae died on the 4th day.

3.2.18. Pinaceae

Coniferous forests are very common in the southern Himalayas, usually huge trees with a height of tens of meters. When tested with ten larvae, *Keteleeria evelyniana* was rejected outright.

3.2.19. Rutaceae

Plants in the genus *Zanthoxylum* were found in the habitat of *S. bouyeri* in Mêdog, therefore, *Zanthoxylum armatum* was tested as a host for ten larvae. Only minimal bite marks were observed after two days, and 4 larvae had starved to death on the 3rd day. The plant was finally considered to be rejected, and the remaining larvae were transferred to other plants for testing.

3.2.20. Vitaceae

The family Vitaceae was observed throughout the Tibetan habitats of *S. bouyeri*, but the vine *Parthenocissus semicordata* was rejected by all ten larvae.

3.2.21. Nyssaceae

A representative of Nyssaceae, *Nyssa sinensis*, was accepted by ten larvae, but all of them died in L_1 on the 7th–9th day.

3.2.22. Symplocaceae

A few plants of *Symplocos paniculata* were found to grow naturally in the same region as *S. bouyeri*. Ten larvae readily accepted the plant within a day and produced feces. However, since only a seedling of the plant was near the experimental site, the indoor experiment had to be terminated on the 3rd day.

3.2.23. Theaceae

The evergreen shrub *Camellia sasanqua* was accepted by ten larvae on the 2nd day after hatching. However, the gnawing marks on the edges of the leaves weren't obvious, and larvae actively left the host plant on the 3rd day and did not return to the plant on the 4th–5th days. Eventually, they starved to death in the cage.

3.2.24. Coriariaceae

Initially, only ten larvae were tested with *Coriaria nepalensis* (Fig. 9A), but surprisingly, they exhibited most growth during the first three days as compared to all other groups of larvae. Therefore, a second group was established, comprising 43 larvae that had hatched on the same day.

Larvae of the second, larger group had had a later hatching date than the ten larvae in the first group, but all individuals in L_2 entered the pre-molting state on the same day (21 Jul. 2022). During L_4, the ten larvae from the first and 23 larvae from the second group were released outdoors on 04 Aug. 2022. One of the remaining 20 larvae was killed for morphological studies during L_5, while the remaining 19 larvae completed their larval instars successfully and pupated in the soil. Apart from slight differences in the size of mature larvae, possibly due to gender, larvae across all groups reared on *C. nepalensis* maintained perfect developmental consistency during their $L_{1–4}$, with none of the larvae leaving the host plant restlessly before feeding ended. The mature larvae were very strong and fully expressed some of their biological habits. Details of their complete larval development are given in Table S1.

3.2.25. Phyllanthaceae

Ten larvae were tested with *Bischofia polycarpa*, which they fed on quickly. However, the larvae didn't grow and finally died within a week.

3.2.26. Oleaceae

This plant family is widely used to rear larvae of many saturniids in captivity from around the world. Six larvae were presented with *Ligustrum lucidum*, but all individuals died during the 3rd–4th day after feeding.

3.3. Ecological monitoring

Mêdog is located on the southern side of the Himalayas, and was the main area where *S. bouyeri* was collected.

Figure 9. A A cluster of *Coriaria nepalensis* growing naturally in northern Kunming at 1996 m; scale bar = 40 cm. **B** Integumentary fluorescence of *Sinobirma bouyeri* L_5 under 365 nm UV, dorsal view; scale bar = 3 mm. **C** Egg parasitoid wasp of *Sinobirma bouyeri*, dorsolateral view; scale bar = 500 μm.

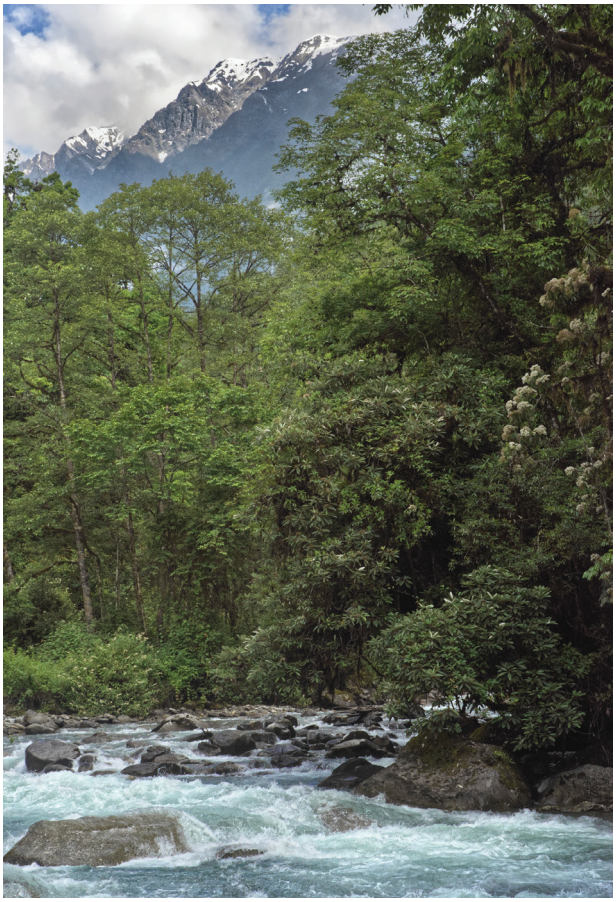

Figure 10. The natural habitat of *Sinobirma bouyeri* in southeastern Himalayas. Mêdog County, Tibet Autonomous Region, China, 2145 m. 25 Jun. 2023.

At this locality, these moths were observed under lamps at altitudes of 1953–2150 m in valleys (Fig. 10). While no traps had been set at lower elevations, no adults of the species were trapped between 2845 m and 3188 m in late June 2021.

During surveys at 1300–2400 m, local Lhoba people confirmed that there was snow cover every year in December and January. A total of 6,707 outdoor climatic data points was collected in Mêdog at 2134 m during 19–26 June 2022 (Table S2). Temperatures ranged from 14.3 to 27°C (average: 18.4°C), while relative humidity ranged from 54.2 to 98.7% (average: 89.4% RH).

3.4. Observations on behaviors

All data of times mentioned in the sections 3.4.1–3.4.4 are based on UTC+8.

3.4.1. Adults

Unfortunately, the precise time of flight of each individual wasn't recorded during light collecting, but the adults arrived at the light within three hours after full sunset (locally ca. 21:00). The moths are inactive during the day unless disturbed, and their eye spots on the hindwings are usually covered by the forewings while at rest (Fig. 11A, C), but displayed when excited or frightened (Fig. 11B). In absence of external disturbance, oviposition occurred only at ca. 22:00–23:30 each night. Almost all females clang to the inside of the cylindrical net-cage top (Fig. 11D, E), protruded their papillae anales [ovipositor lobes] through the meshes and deposited their eggs onto the external surface of the cage (Fig. 11E, F). Only a small number of eggs was deposited on the inner surface or on the external surface of the lateral wall, and none were laid on the cage bottom. Female moths rarely laid eggs in tight enclosures (such as triangle envelopes), the ovipositional behavior requires a relatively large space. The females in this study survived 4–6 days in the cage after having been captured, while males lived around 1–4 days.

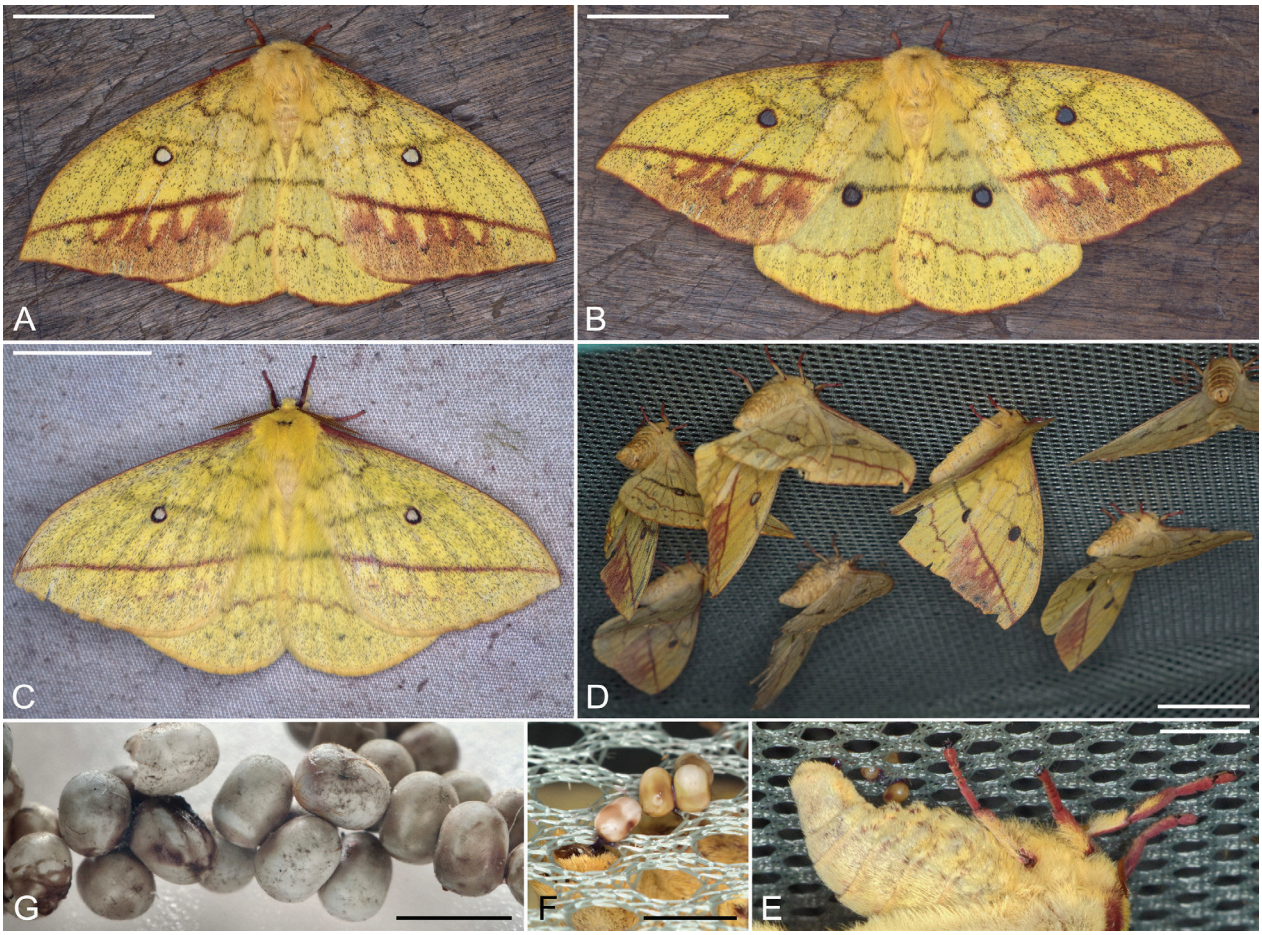

Figure 11. *Sinobirma bouyeri*. **A–E** Adults; **F–G** ova. **A** ♀, resting position, dorsal view, scale bar = 20 mm. **B** ♀, startled, dorsal view, scale bar = 20 mm. **C** ♂, resting position, dorsal view, scale bar = 20 mm. **D** Pre-oviposition, scale bar = 20 mm. **E** Oviposition, scale bar = 5 mm. **F** Oviposition, scale bar = 3 mm. **G** Ova, scale bar = 2 mm.

3.4.2. Ova

Because the abdominal tip of female moth couldn't move freely while passing through the cage mesh, the ova attached on the external surfaces of the cage usually formed irregular clusters. However, the ova collected from the inner surfaces of the cage were arranged side by side into parallel and single–tiered rows, in some cases overlapping into orderly clusters of 2–6 tiers. A total of 419 eggs was oviposited during 21–29 Jun. 2022. Only 53 ova remained unhatched by 25 Jul. 2022, ten of which were randomly dissected, yielding six relatively well–developed larval embryos (head capsules were visible), while the remaining four were undeveloped liquid.

3.4.3. Larvae

A total of 366 larvae hatched successfully from the eggs at 07:00–14:00 during the dates 05–12 Jul. 2022. Spraying water onto the egg shells is one of the key stimuli for larval eclosion. Processionary behavior was observed during $L_{1–4}$ of *S. bouyeri* (e.g., Fig. 12B), and fresh L_1 usually moved slowly in single file (sometimes forming a closed ring) as soon as they hatched. These larvae always formed clusters, with the largest one observed consisting of 147 individuals that hatched on 06 Jul. 2022. They did not aggregate closer to the light source and thereby didn't indicate positive phototaxis. When a $L_{1–4}$ larval cluster formed, all individuals oscillated their heads side to side (e.g., File S1) before they rested. Typically, feeding, resting and settling for pre-ecdysis were all synchronized within a $L_{1–4}$ cluster (Fig. 12B–H). The only exception were single larvae in the rearing group of *P. cerasoides*, which occasionally left their cluster to feed on another leaf.

Larvae of different instars and originating from different females aggregated regularly (e.g., Fig. 12D). The aggregation behavior was strong at all larval stages. For example, if a feeding larval cluster was manually dispersed onto different stems of the plant, the larvae would quickly reform a single or multiple clusters, with a minimum of two larvae. The strong drive to aggregate also resulted frequently in larvae crawling on top of each other. In $L_{4–5}$, when disturbed during feeding, larvae were retracting the upper part of the larval head capsule into T_1.

From L_1, the larvae fed on leaves by starting from the edges, rather than gnawing a hole into the surface. They were not observed feeding on stems, except for a few L_5. Larvae showed different degrees of the feeding behavior during day and night. The leaves of *C. nepalensis* are relatively small, but the larval groups could aggregate on the undersides of the leaves from L_1 to early L_4.

Figure 12. *Sinobirma bouyeri*. **A** A cluster of fresh L_1 (with ova and eggshells), dorsal view, scale bar = 6 mm. **B** Processionary L_1 rebuilding the cluster on *Lagerstroemia indica*, dorsal view, scale bar = 5 mm. **C** A cluster of pre-molting L_1 on *Prunus cerasoides*, dorsal view, scale bar = 6 mm. **D** A cluster of $L_{1–2}$ resting on *Salix babylonica*, scale bar = 5 mm. **E** A cluster of L_2 feeding on *Coriaria nepalensis*, dorsal view, scale bar = 10 mm. **F** A Pre-molting L_2 moving and rebuilding their cluster on *P. cerasoides*, lateral view, scale bar = 5 mm. **G** A cluster of L_3 feeding on *P. cerasoides*, dorsal view, scale bar = 10 mm. **H** A cluster of L_4 resting on *C. nepalensis*, dorsal view, scale bar = 10 mm. **I** A cluster of L_5 resting on the lower parts of the stems of *C. nepalensis*, dorsal-lateral views, scale bar = 10 mm.

Starting with the late L_4, due to their larger size, the strategy changed into clustered resting during the day and dispersed feeding at night. This is a circadian rhythm relates to negative phototaxis of the mature larvae. All 19 L_5 in the *C. nepalensis* test group strictly formed a united cluster on the lower parts of the plant stems during the

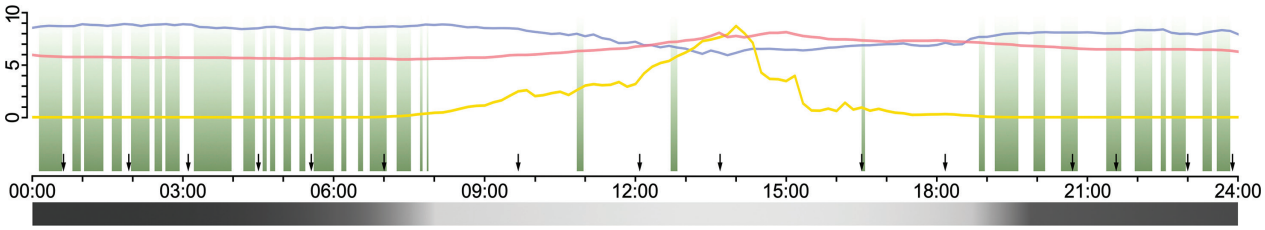

Figure 13. 24 hours (05 Sep. 2022) continuous observation of a single *Sinobirma bouyeri* L_5 (Table S3), reared on *Prunus cerasoides*. Green bars = the time periods of larval feeding. Black triangles = the moments of larval defecation. Red line = temperature (°C). Blue line = humidity (RH%). Yellow line = illumination (Lux). The ordinate on the left is for polylines only (data sampling interval 10 minutes), 1 scale tick = 3°C = 8 RH% = 800 Lux. Scale bar at bottom visualizes illumination, with the darker parts representing night and the light gray day.

day, without any feeding and processionary activities (Fig. 12I). If water was sprayed onto the vegetation, some larvae would move slowly in small areas to drink, without leaving their cluster. After sunset, these larvae began to disperse to different leaves, feeding individually until sunrise. At sunrise they quickly formed a new cluster on the lower stems and remained quiescent. The test group maintained their perfect rhythmic uniformity until their feeding ended.

Because the leaves of *P. cerasoides* are relatively larger and because of the uneven development of the 17 larvae in this test group, some larger L_5 used to rest together on the lower stems during the day and to disperse to feed on leaves during the night. Sometimes 2–4 smaller larvae (during L_5 or L_6) aggregated on the undersides of leaves, but rarely fed by day (only about 0–2 times of feeding, one lasting less than 10 minutes); they mainly fed at night.

As an experiment, a stronger larva from the cauline larval cluster was selected and moved to a separate plant of *P. cerasoides* to record its feeding and defecation times over 24 hours (Fig. 13; Table S3). Its feeding activity was predominantly at night, while it fed only three times during the day for durations of ca. 4–8 minutes.

It is worth mentioning that the green parts of the mature larval integument appeared weakly fluorescent under ultraviolet excitation, while the black and yellow parts were non-fluorescent. In the tests, the fluorescence visible to human eyes were the strongest under 365 nm UV (Fig. 9B), but under 313 nm UV and 254 nm UV the characteristics were relatively weaker. No other larval instars other than L_5 were tested for fluorescence.

Scoli of $L_{1–5}$ of the species had no apparent defensive function, and there was no irritant or urticating reaction upon contact with my skin. Most saturniid larvae rest with their thoracic legs lifted from the plants and hanging in the air, sometimes including the prolegs $A_{3–4}$, but all larvae of *S. bouyeri* always firmly grasped the host plant with all legs and prolegs while at rest. The larvae would secrete a small amount of silk on the vegetation to anchor their crochets before entering each pre-molting period. The pre-molt larvae maintained the ability to move vigorously, and if necessary, they even changed the position of each individual within a cluster (e.g., Fig. 12F). Most larvae fed first on their shed cuticles after ecdysis (except the head capsule).

The midgut appeared brownish red externally in L_1 that were raised on *L. indica* and *P. cerasoides*, but appeared bright green in L_1 on *S. babylonica* and *C. nepalensis*. The final feces [frass] of all individuals that fed on *C. nepalensis* were dark green (Fig. 14C), while those of all individuals that fed on *P. cerasoides* were dark brownish red (Fig. 14A, B). After feeding had ended, their gut-cleansing behavior occurred almost exclusively during the morning (09:00–12:00), and only one specimen raised on *C. nepalensis* produced its final feces around midnight. After that, larvae showed no longer clustering behavior and left their cluster. Most of these larvae fell directly from their host plant to the ground due to rapid movement, but a few larvae crawled down the stems. When larvae reached the ground, they still moved quickly and restlessly for about 10 hours, before they burrowed into the soil at night (Fig. 14D). At this point, their scoli D-III and SD-III were pointing more posteriorly making it easier to enter the soil (Figs 14D, 15).

3.4.4. Pupae

A total of 15 males and 19 females pupated in the soil at 6–12 cm depth (the distances from pupa to the upper surface of the moss-layer). The weights of pupae reared on *P. cerasoides* were 1.23–1.74 g for males (average: 1.61 g) and 1.53–2.27 g for females (average: 1.90 g), respectively. In contrast, those that fed on *C. nepalensis* weighed 1.56–2.15 g for males (average: 1.95 g) and 2.03–2.66 g for females (average: 2.32 g), respectively (Table S4).

From all rearings, only one natural tunnel was retained in its entirety, with the inside of it slightly collapsed from excavating pupae. The longitudinally sectioned tunnel was photographed after repairing it (Fig. 14H). The cross-section of the tunnel was circular, as shown by the remaining boreholes on the surface (e.g., Fig. 14E, F).

Each pupa was surrounded by a gap of ca. 1–3 mm between pupal shell and soil (Fig. 14G, H). The wall of the pupal chamber was loose, irregular and shapeless, and like the tunnel without any reinforcement. All pupae were oriented transversely or nearly vertically, with their head facing or parallel to the upper surface of the soil (Fig. 14G, H).

3.5. Parasitoid

Unhatched ova of *S. bouyeri* were stored in a plastic zip lock bag at room temperature (ca. 19–24°C) from 25 Jul. to 3 Sep. 2022. A dead minute wasp found in this bag is

Figure 14. *Sinobirma bouyeri*. **A–C** Final feces of L_5, reared on *Prunus cerasoides* (**A**), *P. cerasoides* (**B**) and *Coriaria nepalensis* (**C**), scale bars = 10 mm. **D** L_5, burrowing into the soil after feeding had ended, lateral view, scale bar = 10 mm. **E** Entrance of larval borehole, covered with moss, scale bar = 5 mm. **F** Tunnel entrance after removing the moss in E, scale bar = 5 mm. **G** Fully tanned pupa ♀, ca. 9 cm from the upper surface of the moss-layer and its head is orienting upward to this surface, scale bar = 10 mm. **H** Freshly molted and incompletely tanned ♀ pupa, ca. 10 cm from the upper surface of the moss-layer, scale bar = 20 mm.

the only egg parasitoid recorded for the genus *Sinobirma* so far:

Single ♀ wasp (Fig. 9C): Head, thora, abdominal segments and coxae mainly shiny black; femur, trochanter, tibia and tarsus brown, mostly on the medial areas. Antenna near black, except for the anterior parts of the scape and pedicel, which are dark brown. Antennal flagellum 9-segmented, with the apical 5 flagellomeres forming an

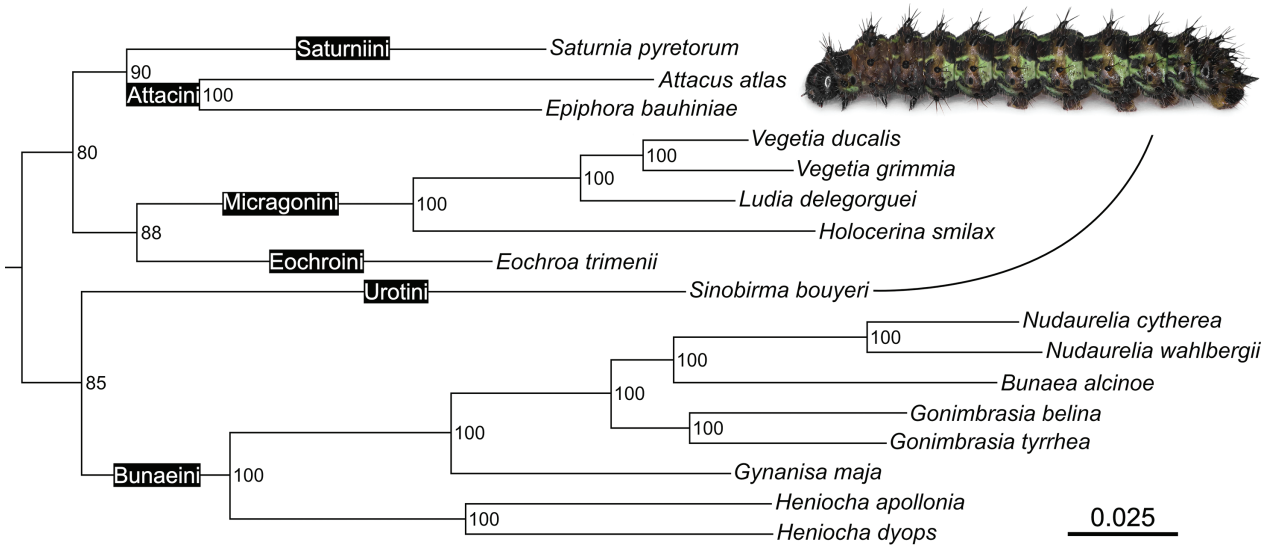

Figure 15. ML phylogeny of the family Saturniidae (part) based on 13 mitochondrial PCGs. Ultrafast bootstrap values to the right of each node, outgroup Bombycidae not shown. The larval image is of a L_5 of *Sinobirma bouyeri* that ended feeding.

enlarged club. Median ocellus located anterior to lateral ocelli, the latter close to inner orbits. Forewing with clear costal, postmarginal and stigmal veins, but only the costal vein is visible in the marginal area of the hindwing.

3.6. Mitogenomics

The topologies of the ML trees calculated in both MEGA X and IQ-TREE were exactly the same. The topological relationship is (((Saturniini + Attacini) + (Micragonini + Eochroini)) + (Urotini + Bunaeini)) + outgroup (Fig. 15). All nodes within tribes have ultrafast bootstrap values of 100%, while nodes between tribes are only weakly supported with 80–90%.

4. Discussion

The evolutionary relationships of *Sinobirma* and its relatives have been discussed controversially in literature. When establishing the genus *Maltagorea*, Bouyer (1993) related *Maltagorea* to *Tagoropsis* and *Pseudantheraea*, proposing them to form a monophyletic group. Based on comparison of adult morphology, *Sinobirma* has also been regarded as belonging to this group (Nässig and Oberprieler 1994; Rougerie 2003; Rougerie et al. 2012). Adding larval and pupal characteristics, Oberprielder (1997) suggested to include also the African genera *Pseudaphelia* Kirby, 1892, *Pselaphelia* Aurivillius, 1904 and *Urota* Westwood, 1849, while he considered *Eudaemonia* Hübner, 1819, *Antistathmoptera* Tams, 1935, *Usta* Wallengren, 1863 and *Parusta* Rothschild, 1907 to be of uncertain status. This deviated from the widely known and traditionally used classification in the monograph by Bouvier (1936: 29–32), which included the latter four African taxa and several of the above genera in a joint tribe "Pseudapheliicae". The question of which genera should be included in this tribe were also debated by Racheli and Racheli (2006).

To elucidate the origin of *Sinobirma* further, this discussion is focused on comparing morphological and biological characteristics between *Sinobirma bouyeri* and genera that have been proposed as close relatives. Additional independent molecular evidence from mitochondrial DNA is also discussed.

4.1. Preimaginal morphology

At present, the putative sister genera of *Sinobirma* still lack microscopic morphological observations on ova for comparison with *Sinobirma*. The egg chorion of *Pseudantheraea discrepans* (Butler, 1878) shows a fine reticulation at 24x magnification (Seydel 1939), while Bouyer et al. (2004) described the ova of *Pseudantheraea imperator* Rougeot, 1962 as more than twice the size of those of *P. discrepans*, and figured the ova of the latter in color. Although images of the eggs of *S. malaisei* (Rougerie et al. 2012) and *Tagoropsis flavinata* (Walker, 1865) (Lampe 2010: 41) were published, all of them looked off-white in color and the shapes are very close to *S. bouyeri*, based on macroscopic views.

Similarly to eggs, very little is known about the early larval instars of the relatives of *Sinobirma*. The L_1 of *S. malaisei* appear almost indistinguishable from those of *S. bouyeri* as illustrated in Rougerie et al. (2012), except maybe by the absence of gray spots around scoli D of T_2–A_9 in the former (Rougerie et al. 2012). In contrast, the light gray spots are more conspicuous between pairs of scoli D-III in most examined L_1 caterpillars of *S. bouyeri*, though nearly impossible to observe in some specimens (e.g., Fig. 12C). Both species have very large and shiny prothoracic shields during L_1.

Rougerie and Estradel (2008) provided an important larval observation involving species within several pu-

tative or potential sister genera of *Sinobirma*, including *Maltagorea vulpina* (Butler, 1882), *Maltagorea fusicolor* (Mabille, 1879), *Usta angulata* Rothschild, 1895 and *Parusta thelxinoe* Fawcett, 1915. The L_1 of these four species were described as having 2 primary setae borne on each XD, which is a trait also clearly shown in each larval instar of *S. bouyeri*. Rougerie and Estradel (2008) also mentioned that the setal quantities of scoli SV of $T_{1–3}$ of *M. fusicolor* L_1 are "4-3-3", which is the same as for the $L_{1–5}$ of *S. bouyeri*. Chalazae/Scoli SV were reported for T_1–A_9 of the larvae of *Tagoropsis genoviefae* Rougeot, 1950, *P. discrepans* and *M. fusicolor* (Rougerie and Estradel 2008), and these examples appear similar to *S. bouyeri*.

Lampe (2010: 41) and Staude et al. (2016: S37–S38) figured photographs of the larvae of *T. flavinata*. The L_1 larval black prothoracic shields and head capsule, and the yellow ground color of T_1–A_{10} of *S. bouyeri* look very similar to the L_1 of *T. flavinata*. More importantly, the scoli D of T_2–A_9 appear to be morphologically similar in both species, being of an asterisk-like type, especially in the mature instar (L_5). They also share high bases that bear spiny setae outwardly elongated toward multiple directions. This shared character was also illustrated for the scoli D of *T. genoviefae* by Rougeot (1955: 40).

In the L_5 of *T. flavinata*, the sclerotized parts (mainly the head capsule, prothoracic shield, anal shield, legs $T_{1–3}$, lateral plates of prolegs $A_{3–6}$ and A_{10}, bases of scoli SV, L, SD, D and XD) are of similar colors near red-orange. In contrast, the same areas of fresh L_5 of *S. bouyeri* are all bright yellow just after ecdysis (Fig. 7I), but then turn into shiny black as the larva hardens. This suggests that the integumentary systems of the genera *Tagoropsis* and *Sinobirma*, especially their sclerites may have comparable biochemical characteristics.

The largest segments are always $A_{3–4,}$ for *S. bouyeri* $L_{2–5}$, making the larva as a whole shaped cylindrical but slightly tend to fusiform. As mentioned above, when the larvae were in a physically relaxed state, the dorsal area of the junction zone between A_1/A_2 appeared to be the most sunken area in lateral view, especially in $L_{2–5}$ (Fig. 7C, E, G, J). A similar sunken junction zone between A_1/A_2 appears to be present in *T. flavinata* $L_{1–5}$. Based on illustrations in Lampe (2010) and Staude et al. (2016), mature larvae of *Pseudaphelia apollinaris* (Boisduval, 1847), *Urota sinope* (Westwood, 1849), *Usta wallengrenii* (C. & R. Felder, 1859) and *Usta terpsichore* (Maassen, 1885) also appear to have obvious depression of the junction zone between A_1/A_2 in lateral view. In addition, the macroscopic forms of *T. flavinata* $L_{1–5}$ also show intumescent $A_{3–4}$ similar to *S. bouyeri*.

The bases of the paired scoli D-III are medially fused on A_8 in *S. bouyeri*. This character is also present in *T. flavinata* as described by Packard (1914: 166) and in *Tagoropsis hanningtoni* (Butler, 1883) as figured by Seydel (1939). Furthermore, the original description (Rougeot 1950) of the larva of *T. genoviefae* explicitly noted the same fusion on dorsal A_8.

One noteworthy feature of *S. bouyeri* is the flattened A_{10} in lateral view of $L_{1–5}$, with the posterior margins of the pair of lateral plates of the anal prolegs usually combined to form a minor arc outline in dorsal view. This means that the opening angle between the two anal prolegs is very flexible, whereas it is usually in a horizontal state (nearly straight line). This structure is presumably suitable for crawling and clustering on the smooth surfaces of the undersides of leaves.

Furthermore, the triangular anal shields of $L_{4–5}$ of *S. bouyeri* are all drawn out to form a pointed posterior tip, a feature shared with the mature larvae of *T. genoviefae* (Rougeot 1962: 70), *T. hanningtoni* (Lampe 2010: 42) and *T. flavinata*. The anal shields of these three species are triangular in shape, with a drawn-out posterior tip of relatively small size, while *U. sinope* (Staude et al. 2016: S37–S40) and *M. auricolor* (Rougerie 2005: fig. 449; Basquin 2015) appear to have a more reduced posterior tip of their A_{10}. A comparable structure is also present in *P. apollinaris* (Staude et al. 2016: S37–S38) and *Pselaphelia flavivitta* (Walker, 1862) (Lampe 2010: 43), with their anal shields drawn out to form a very long spine pointing posteriad, more pronounced than in *S. bouyeri*. Oberprieler (1997) considered these similar anal shields potentially a distinctive feature shared by the group comprising *Pselaphelia*, *Pseudaphelia*, *Tagoropsis* and *Urota*.

For *S. bouyeri*, each scolus D-II on the anal shield bears 2 primary setae during $L_{1–5}$. A similar trait had been known to occur in some other members of the tribe Urotini, but also in other African tribes (Rougerie and Estradel 2008).

The pupal shell of *S. bouyeri* has three pairs of dorsal thoracic tubercles of large sizes, and a very long, spiny cremaster on the tip of A_{10}. Seydel (1939) described the pupa of *T. hanningtoni* as having a total of six tubercles borne on the dorsal area of thoracic segments and the pupa ending with a pointed cremaster, very much like the pupal painting of *T. flavinata* illustrated by Cooper and Cooper (2002: 49). The green pupa of *P. discrepans* figured by Rougeot (1955: Pl. 1), Gardiner (1982: Pl. 20) and Lampe (2010: 40) shows the same distribution of dorsal thoracic tubercles as *S. bouyeri*, and the former species has an elongated cremaster with hooks. The pupa of *M. auricolor* (Rougerie 2005: fig. 513) appears to have a similar spined tip on A_{10}, but attenuated to being relatively shorter than in *S. bouyeri*. Also *M. fusicolor* has an extended cremaster that was observed to have two terminal hooks (Bouvier 1936: 39–40: "*Tagoropsis subocellata*"). In fact, Oberprieler (1997) mentioned that both genera *Tagoropsis* and *Pseudantheraea*, as well as *Pselaphelia*, *Pseudaphelia* and *Urota*, all have comparable pupae based on their elongated cremaster. Furthermore, each of the spiracles of T_1 and $A_{2–8}$ of *S. bouyeri* is protected within a cavity under an elliptic annular cap. Rougerie and Estradel (2008) observed similar characters for the pupal spiracles of *M. auricolor*, *Maltagorea monsarrati* (Griveaud, 1968), *M. fusicolor*, *T. genoviefae* and *P. discrepans*.

While multiple potential sister genera share the aforementioned morphological features with *S. bouyeri*, differences in structural detail exist between them. For examples, images in the above literature show that scoli D of T_2–A_9 appear spine-like and strongly elongated in the

mature larva of *P. discrepans*, with lateral margins of the anal shield curved. Larvae of *M. auricolor* and similarly *M. fusicolor* (illustrated by Paulian 1953 as "*Copaxa subocellata*") have more reduced scoli D and SD on T_2–A_9 than *S. bouyeri*. Moreover, *M. auricolor* has only one pair of dorsal thoracic tubercles borne on pupal T_3, a feature that differs from *Tagoropsis*, *Pseudantheraea* and *Sinobirma*, which have a total of three pairs on $T_{1–3}$, respectively.

The trait of medially fused scoli D on A_8 has been known to be shared by larvae of *Tagoropsis* spp., *S. malaisei* and *S. bouyeri*, but *M. auricolor* and *P. discrepans* hatch with a pair of scoli D on A_8 that are completely separated from each other. Rougeot (1950) had suggested this to be an important character to distinguish the genera *Tagoropsis* and *Pseudantheraea*. Moreover, the mature larvae of *P. apollinaris* and *P. flavivitta* have reduced scoli D and SD, appear to have a triangular prothoracic shield with a drawn-out anterior tip, and extended lateral margins that form a wider shape in dorsal view. All of these features make these larvae resemble the Asian genus *Salassa* Moore, 1859, whose larvae are well-known examples of leaf-mimicing. However, the study by Rougerie (2005: 293) supports the hypothesis of evolutionary convergence between the two African genera and the Asian *Salassa*.

Mature larvae of *U. wallengrenii* and *U. terpsichore* do not have an elongated posterior tip of the anal shield, and the pupa of the former species has a posterior elevated crest in annular shape on $A_{4–6}$. These characteristics also appear in the pupa of *U. angulata* (Rougerie and Estradel 2008). Nässig et al. (2015) suggested that the genus *Usta* may have a more distant relationship to the core group containing *Sinobirma*, while Rougerie et al. (preprint) assigned both *Parusta* and *Usta* to the tribe Eochroini with strong support. This is contrary to Pinhey (1956: 26), who considered the genus *Parusta* to be potentially closely related to *Pseudaphelia*. The genera *Eudaemonia* and *Antistathmoptera* are not considered in this section due to obvious adult differences to *Sinobirma* (e.g., Oberprieler 1997).

Although the color combinations of the final larval instar of the above related African genera do not have similar patterns to *S. bouyeri*, coincidentally, the colors of the mature larva of the Australian *Opodiphthera astrophela* (Walker, 1855) are similar, especially in the painting in Scott (1890). Similarly, mature larvae of *Saturnia centralis* Naumann and Löffler, 2005 are also superficially similar to *S. bouyeri* (Liu and Peigler 2021), because integuments of both species are black grounds studded with green patches and stripes. They also share obvious aggregation behavior during larval instars. If Felix Bryk had encountered the mature larva of *Sinobirma* 80 years ago, he might have felt certain of the "close relationship" of *Sinobirma* to these other genera. However, such color patterns (black or dark brown grounds, with vivid green stripes or patches on especially the lateral areas) occur in different genera or even subfamilies of Saturniidae, representing most probably examples of convergent evolution.

Despite all the similarities and differences, further data from African species would be needed to identify which characters are informative to reconstruct a morphology-based phylogeny. At present, our knowledge of the above genera is incomplete, and especially detailed morphological and biological work involving ova, larvae and pupae are rare. Nevertheless, Nässig and Oberprieler (1994) and Rougerie et al. (preprint) postulated that *Tagoropsis*, *Pseudantheraea*, *Maltagorea* and *Sinobirma* form a closely related group with similar morphology and genes. The preimaginal stages of *S. bouyeri* further support this hypothesis. Out of these genera, the larvae of *Sinobirma* are morphologically most similar to *Tagoropsis*, especially due to their highly similar scoli D (form and fusion) and anal shield. Likewise, pupae of the two genera are more similar to each other than compared to other genera. Although Cooper (2002: xiv) explicitly classified these four genera in the new tribe "Tagoropsini" and excluded *Urota*, the larval characteristics combined with adult morphology indicate that *Urota* is more likely to be the sister taxon of the above core group ("Tagoropsini"). Unlike *Tagoropsis*, *Pseudantheraea*, *Maltagorea* and *Sinobirma*, the larva of *U. sinope* looks stubbier, rather than an elongated cylinder, which is caused by the middorsal areas of T_2 and T_3 being swollen and elevated. Furthermore, the scoli D of T_2–A_9 of *U. sinope* are noticeably reduced to rounded, pimple-like structures.

4.2. Preference of feeding

Exploring the plants that *Sinobirma* accepted or rejected can provide insights into its ecological niche. Previously, only Rougerie et al. (2012) reported that *S. malaisei* L_1 failed to rear on *Prunus cerasifera* (Rosaceae). In addition, Rougerie (2003) mentioned that at the biotope of *S. malaisei* in western Yunnan, the vegetation including many flowering *Castanopsis* (Fagaceae).

This study tested host plant acceptance by *S. bouyeri* systematically. Plants completely rejected by the larvae of *S. bouyeri* came from the families Ericaceae, Malvaceae, Lauraceae, Betulaceae, Magnoliaceae, Pinaceae, Vitaceae and Santalaceae. Similarly, there were minute bite marks, but the larvae did not continue to feed and even starved to death when attempted to rear on Meliaceae, Rutaceae and Theaceae.

Altingiaceae seems to be a special case where within a group some larvae clearly accepted but some totally rejected the offered host plant, thereby separating two dinstict larval clusters in the rearing container. Ultimately, none of the larvae developed on this host. Similarly, *S. bouyeri* rejected two but fed one species within the family Fabaceae, but the accepted plant caused the caterpillars to die consecutively over several days. The same acceptance yet mortality pattern occurred also with Anacardiaceae, Fagaceae, Nyssaceae, Phyllanthaceae and Oleaceae. Even more problematic was the rearing on Sapindaceae and Ulmaceae, which resulted in all individuals of each larval group to die rapidly the same day.

Regrettably, no valid data were available for the group testing on Symplocaceae and it remains unknown whether the larvae of *S. bouyeri* can molt to L_2 or even com-

plete the whole larval stage. This family of plants is rarely reported as a host plant of saturniids, e.g., *A. atlas* was reported to feed on *Symplocos paniculata* in India (Rondot 1887: 68: "*Symplocos crataegoides*"), and *Symplocos tinctoria* is a hostplant for *Callosamia promethea* (Drury, 1773) in South Carolina (Ferguson 1972: 236–237).

Of all the tested host plants, only 5 families of plants were able to support the development of *S. bouyeri* larvae from L_1 molting into L_2. The least suitable plant was *J. regia*, as all larvae died soon after the first ecdysis. This result is consistent with the mortality of *S. malaisei* observed by Rougerie et al. 2012. Larvae feeding on *L. indica* had shown signs that this plant wasn't the right host, i.e., the slow growth of L_2 larvae and increased size differences between individuals. Yet, it cannot be ruled out fully that some individuals of *S. bouyeri* feeding on this plant would have survived to pupation. *Salix* spp. were observed to be cultivated along the country roads in Nyingchi, and there were native plants of this genus growing in the habitat of *S. bouyeri* in Mêdog. However, this plant didn't appear to be a correct host in the natural environments and was also unsuitable for captive rearing, although a fair number of willow-feeding larvae can survive to maturity. Larval feeding on the family Rosaceae was equivocal, with individuals on wild rose revealing continuous mortality over multiple days during $L_{1–2}$, while the group fed on *P. cerasoides* completed all larval instars.

Of all the plants tested, *C. nepalensis* in the family Coriariaceae is the best host plant for *S. bouyeri*. There were no larval losses from hatching to the last larva burrowing into the soil, and the developmental duration was almost a month shorter than that of larvae fed on *P. cerasoides* (Table S1). As a shrub (Fig. 9A), *C. nepalensis* is widely distributed in the humid regions of southern provinces of China and the Sub-Himalayas (Min and Brach 2008). Host testing showed that most of the plants rejected by *S. bouyeri* were tall trees in nature. The dark integument of the mature larvae and its feeding habit at night indicate that *S. bouyeri* inhabits the understory, and the true host plants in this biotope may be shrubs and vines. *C. nepalensis* would fit such requirements.

Of the genera that are closely related to *Sinobirma*, *Tagoropsis* occurs only on the mainland of Sub-Saharan Africa and was long known to feed on Sapindaceae. An early report by Schultze (1914) noted that *T. flavinata* fed on *Allophylus africanus* in the wild in Cameroon. In South Africa, larvae of *T. flavinata* were recorded as feeding on the same plant (Platt 1921: "*Schmidelia africana*"; Pinhey 1972: 54: "*Allophylus melanocarpus*"). More recently, *Allophylus natalensis* and *Allophylus dregeanus* were listed as host plants of *T. flavinata* (Cooper and Cooper 2002: 48; Staude et al. 2016: S37). Working in then French Congo, Seydel (1939) published a record of *A. africanus* used to rear *T. hanningtoni*, for which Crotch (1956: 148) also suggested "might be tried on maple and sycamore". Santin (2004) listed *Malus* (Rosaceae) for *T. hanningtoni*, while Meister (2011: 131) added *Bauhinia* (Fabaceae) for the same moth, with the records of *A. africanus* for *T. genoviefae*, *T. hecqui* Bouyer, 1989, *T. rougeoti* Fletcher, 1968 and *T. sabulosa* Rothschild, 1907.

Pseudantheraea is a polyphagous genus occurring in central-western Africa, feeding on multiple botanical families in the wild. *Poga oleosa* (Anisophylleaceae) and *Uapaca guineenis* (Phyllanthaceae) were recorded as natural hosts of *P. discrepans* in Gabon, while the genus *Terminalia* (Combretaceae) was accepted in captivity (Rougeot 1949; Rougeot 1962: 75). Moreover, Gardiner (1982: 199) listed *Mangifera indica* (Anacardiaceae) for the same species. *Salix caprea* (Salicaceae) was observed to be accepted by *P. discrepans* (Bouyer et al. 2004). In the captivity in Germany, the larvae of *P. discrepans* were further listed as feeding on *Caloncoba welwitschii* (Achariaceae), *Coelocaryon botryoides* (Myristicaceae), *Ricinodendron heudelotii* (Euphorbiaceae), *S. babylonica* and *Fagus* (Fagaceae), whereas its sister species *P. imperator* possibly accepted the genera *Fagus*, *Mangifera*, *Terminalia* and *Uapaca* (Meister 2011: 130). *P. discrepans* has been reported as an edible insects in Angola (Lautenschläger et al. 2017) and Congo, and people in the latter country recently supplemented the list of accepted host plants with *Entandrophragma candollei* (Meliaceae), *Spondias dulcis* (Anacardiaceae), *Spondias mombin* (Anacardiaceae) and *Staudtia kamerunensis* (Myristicaceae) (Mabossy-Mobouna et al. 2022).

Maltagorea is restricted to Madagascar and lacks detailed preimaginal reports. Larvae of *M. fusicolor* have been known to feed in the wild on the tapia tree *Uapaca bojeri* (Phyllanthaceae) (Oberthür 1916: "*Syntherata cambouei*", "*Tapia Edulis* (ou *Chrysopia* sp.?) [sic]"), Euphorbiaceae (Paulian 1953) and *Agauria* (Ericaceae) (Griveaud 1961: 26: "*Tagoropsis subocellata madagascariensis*"); Meister (2011: 129) also listed *Aguiaria excelsa* (Malvaceae) as a host plant. *M. auricolor* feeds naturally on *U. bojeri* (Basquin 2015).

As mentioned above, a further seven African genera *Urota*, *Pseudaphelia*, *Pselaphelia*, *Eudaemonia*, *Antistathmoptera*, *Usta* and *Parusta* have been considered as relatives of *Sinobirma* to varying degrees in different works. According to the comprehensive catalogues of the host plants of Saturniidae by Stone (1991), Rougerie (2005) and Meister (2011), the above African genera primarily exploit the families Meliaceae, Zingiberaceae, Lauraceae, Combretaceae, Anacardiaceae, Fabaceae, Myrtaceae and Burseraceae.

More rigorous comparative conclusions could not be drawn as it wasn't possible to test the host plants of all of the above African Saturniidae. Furthermore, it is uncertain whether records in literature resulted in larvae reaching pupation or could even sustain multiple generations. However, polyphagy is here proposed to be a shared trait of the closely related genera *Tagoropsis*, *Pseudantheraea*, *Maltagorea* and *Sinobirma*.

4.3. Ecology of the natural habitats

The natural habitat of *S. bouyeri* in China is recorded here as the Nyingchi area of the Tibet Autonomous Region, a prefecture-level city whose territory contains both northern and southern sides of the eastern Himalayas and

the Yarlung Tsangpo River [upper Brahmaputra]. Bomê [Pome] and Mêdog [Metok] are both counties that belong to Nyingchi, as the type locality. The average annual rainfall of the former region exceeds 800 mm, largely in spring (>300 mm) and summer (>300 mm), with an average temperature of 0–2°C in winter and 16–18°C in summer (Song and Wang 2013: 47, 61–62).

Zheng et al. (2018: 4) reported the average annual rainfall of Mêdog at 2000 m as more than 2200 mm, and average temperatures of 4–6°C in winter and 17–19°C in summer. The area is wet and cloudy, covered with subtropical evergreen broad-leaf forest, which is classified as the notophyllous type in Wolfe (1979: Pl. 1). In vegetation surveys of Tibet, this area was detailed and classified as "Mêdog district, eastern Himalayan tropical evergreen rainforest province, southeastern Asian tropical evergreen or seasonal rainforest region, tropical vegetation zone" by Zhang et al. (1988), with the eco-region named "eastern Himalayan broadleaf forests" of Indomalayan biomes (e.g., Hoekstra et al. 2010: 188–189).

The genera *Tagoropsis*, *Pseudantheraea* and *Maltagorea* are mainly forest and grassland dwellers (Fig. 17), with the predominant climates of their habitats being principally tropical rainforest, monsoon and savanna, but also small areas with oceanic and humid subtropical climates (Peel et al. 2007). In contrast, *Sinobirma* only adapted to the last type. Both *Tagoropsis* and *Maltagorea* tend to be distributed in the highlands of the western and central Somali Plate, while *Sinobirma* is a strictly montane genus which endemics to the northeastern Indian Plate. It suggests that relatively humid climates might have been necessary for the dispersal and distribution of the most recent common ancestor of this core group.

4.4. Biological characteristics

Based on the oviposition behavior described in section 3.4.1, females of *S. bouyeri* may prefer to oviposit in the wild onto surfaces facing the sky (such as the uppersides of leaves or branches), as well as into narrow crevices or pits (such as cracks of stems). This would provide the eggs more exposure to rain and warmth within the understory that's low in sunlight.

Comparing observations made for the $L_{4–5}$ *S. bouyeri* larval groups reared on *C. nepalensis* and *P. cerasoides* (section 3.4.3), it appears that larval cluster size and location on the plant have an influence on the gregarious behaviour. For smaller larvae that inhabited the leaf undersides during the day, the more larvae in a cluster, the more stable the rhythmical feeding-resting behavior was. In contrast, larger larvae that typically clustered on lower stems during the day exhibited the most stable gregarious behaviour. These results are based on only a relatively small number of individuals and observations, and more rigorous experiments are needed in the future to further determine the regulatory role of other factors like light and pheromones in the circadian rhythm of larvae.

Pupation of the mature larvae in captivity was described in detail in section 3.4.4. In nature, soil tends to be substantially more dense and to include more rock particles and plant roots. Therefore, most larval *S. bouyeri* might only burrow to a soil depth of less than 10 cm naturally, but otherwise similarly to the results in section 3.4.4.

Peigler (1999) suggested that pupae and cocoons formed below ground may escape fires. Located at the windward side of the eastern Himalayas, forest floors in Mêdog often experiences accumulation of debris caused by heavy summer and autumn rainfalls. In captivity, larvae had not been observed to reinforce their tunnels and pupal chambers with silk or other measures. Therefore, most pupae in the wild are likely to be completely buried below ground. The pupae of *S. bouyeri* have a long cremaster and spine-like abdominal and head tubercles, with the abdominal tubercles pointing latero-caudad. Presumably, waggling the flexible abdominal segments ($A_{5–7}$) results in rebuilding the pupal chamber and forward movement when the moth emerges. The elliptic annular cap of each spiracle may prevent clogging of the spiracles with soil, especially while pressing against soil for movement.

Rougerie (2003) provided a first biological description of the genus *Sinobirma* in western Yunnan: "Their flight times were remarkably constant, the females arriving at the sheet at about 21:00 and the males between 23:30 and 00:00 local time… *S. malaisei* arrived at the light in an erratic fashion, fluttering around on the ground before settling on the sheet or surrounding shrubs". These observations are essentially consistent with the behavior of *S. bouyeri*.

Cooper and Cooper (2002: 48) described *T. flavinata* in Africa as a "rather weak flier", whose females are readily attracted to car headlights. Likewise, both *P. discrepans* and *P. imperator* are attracted to lights during the night, and statistical data were recorded in detail by Bouyer er al. (2004). *Maltagorea* is also nocturnal, but the flight times of different species within the genus vary significantly (Basquin and Rougerie 2009).

The above publications indicate that some species of the African genera *Tagoropsis*, *Pseudantheraea* and *Maltagorea* have two (or more) flights per year. In contrast, Asian *Sinobirma* is strictly univoltine (see introduction), which is probably an adaptation to the colder Himalayas, but may also correspond to seasonal metabolic rhythms of their natural host plants.

Seydel (1939) described the larva of *T. hanningtoni* as being processionary like Thaumetopoeinae (Notodontidae) and pupating in soil without cocoon. Rougeot (1950) recorded the larvae of *T. genoviefae* as feeding on a shrub called "Evetom [sic]" during the night. He reported that when the larvae stopped feeding, they left the food plant and rested on the ground with help of a few silken threads for pupation, sheltered by leaves or plant fragments. Cooper and Cooper (2002: 48) noted ova of *T. flavinata* having been "laid in arching rows of eggs glued sideways on twigs in up to 7 tiers and the underside of leaves of the larval foodplant". They also reported larvae being "highly gregarious at all instars, moving quickly in single file, head-to-tail, from one position to the next" and "Although the bristles have been said to sting, they have had no effect on us whatsoever... Larvae feed mainly at night spending

the day resting in a clump, often low down, on a thick stem of the larval foodplant" and pupated "among leaf litter on the ground". Nocturnal feeding by larval *T. flavinata* had also been noted already earlier by Bouvier (1928: 531).

P. discrepans has long been known for its peculiar green pupa hanging in a loose cocoon amongst the vegetation (e.g., Holland 1892: "*Saturnia arnobia*"). Bouyer et al. (2004) added that "Larval behavior was characterized by an intensively gregarious habit in all instars. Feeding and resting were nearly always carried out synchronously and in tactile contact. Another unexpected observation was that the larvae always left their feeding site in the late afternoon (around 17 h Central European Summer Time) for approximately one hour and congregated at the neck of the bottle in which the branches were kept".

Oberthür (1916) reported that the pupa of *M. fusicolor* was surrounded by debris and rested between leaves, and Paulian (1953) added that it was naked, protected by loose silk to link together fragments of dry leaves. Bouvier (1936: 40) suggested that such an unformed cocoon revealed its relationship to the genus *Pseudantheraea*. Similarly, Rougerie (2005: fig. 513) figured the pupa of *M. auricolor*, also being protected in a loose cocoon, and Basquin (2015) stated that the species pupated in litter at the base of trees. In contrast, the genus *Maltagorea* still lacks any description of larval behavior.

Considering the above larval characteristics, *Tagoropsis* is the closest genus to *Sinobirma* at the behavioral level. Some species of the two genera are known to have similar larval circadian rhythm and naked, subterranean pupae.

Larval fluorescence has rarely been reported for Saturniidae. Besides *S. bouyeri*, Adès (2007) illustrated larval fluorescence of L_5 of *Actias sinensis* (Walker, 1855), *Actias felicis* (Oberthür, 1896) and hybrid *A. sinensis* ♂ × *Actias dubernardi* (Oberthür, 1897) ♀. Fluorescence occurred primarily at the bases of scoli, with excitation by UV light (peak wavelength 404 nm). Similarly, larvae of *Syssphinx albolineata* (Grote and Robinson, 1866) exhibited fluorescence under UV light, visible on scoli, prothoracic and anal shields, and especially the minute tubercles of the integument (Wagner and Nall 2022). Mature caterpillars of *Citheronia regalis* (Fabricius, 1793), *Eacles imperialis* (Drury, 1773), *Antheraea polyphemus* (Cramer, 1776), *Antheraea compta* Rothschild, 1899, *Actias luna* (Linnaeus, 1758) and *Hyalophora cecropia* (Linnaeus, 1758) have been shown to fluoresce in whole or in part under UV light (Moskowitz 2018; 2021; Liu 2023).

The fluorescent green stripes of *S. bouyeri* L_5 were conspicuous in daylight, which seemed to provide excellent camouflage in vegetation when larvae clustered at the inferior parts of the stems during the day — due to the rainy climate, Sub-Himalayan broad-leaved forest is extensively covered with moss, especially the understory.

4.5. Parasitoid Identification

Using a taxonomic key for the order Hymenoptera (Goulet and Huber 1993), the single saturniid parasitoid wasp in section 3.5 was recognised as belonging to the subfamily Telenominae (Platygastridae). More specifically, the specimen might belong to the genus *Telenomus* Haliday, 1833, which is well-known to parasitise Lepidoptera, and a few genera in this subfamily have been deployed as biocontrol agents (Austin et al. 2005). With parasitic behavior being unlikely to occur indoors (Kunming), this species is most likely a natural parasitoid of *S. bouyeri* in its Himalayan habitat.

4.6. Molecular phylogeny

Nethavhani et al. (2022) published a molecular phylogeny based on the 13 mitochondrial protein-coding genes. The molecular results of the present study detailed in section 3.6 strongly support congruent topologies of the Maximum Likelihood and Bayesian analyses, except for the addition of Urotini in this study (Fig. 16). The new phylogeny supports an African origin of *Sinobirma*, because the tribal clade represented by *S. bouyeri* is sister to Bunaeini — an entirely Afro-Madagascan taxon with high genetic diversity (Kitching et al. 2018). Unfortunately, the genera *Tagoropsis*, *Pseudantheraea* or *Maltagorea* have no complete mitochondrial genomes publicly available at present, and comparative analyses within this group aren't possible yet.

Regier et al. (2008) published a Maximum Likelihood tree based on four protein-coding nuclear gene regions, which demonstrated that the tribe "Urotini" in the traditional sense was polyphyletic. with the "urotine" *Tagoropsis* closest to Bunaeini and the "urotine" *Usta* to Micragonini. Based on the analysis of ultraconserved elements [UCEs], Rougerie et al. (preprint) classified *Usta* as belonging to the re-instated tribe Eochroini, with a restricted, monophyletic tribe Urotini comprising only (((*Pseudantheraea* + *Maltagorea*) + *Sinobirma*) + (*Tagoropsis* + "*Tagoropsiella* Darge, 2008")) + *Urota*.

However, the topologies in these papers (Fig. 16B, C) are congruent at the tribal level, with Bunaeini always closest to Urotini, and together sister to Micragonini + Eochroini, which in turn are sister to Saturniini + Attacini. The topologies based on mitochondrial data, both in Nethavhani et al. (2022) and this study, also support Bunaeini + Urotini, as well as the sistergroup relationships between each Micragonini + Eochroini and Saturniini + Attacini. However, both analyses of miochondrial data place Micragonini + Eochroini as sister to Saturniini + Attacini, albeit with low support, while analyses of nuclear data support Micragonini + Eochroini as sister to Bunaeini + Urotini.

4.7. Evolutionary hypotheses

At first glance, the inclusion of the Himalayan genus *Sinobirma* in the otherwise exclusively African tribe Urotini might seem at odds from a biogeographic perspective and require discussion. Following the phylogeny of Nässig and Oberprieler (1994) and considering the

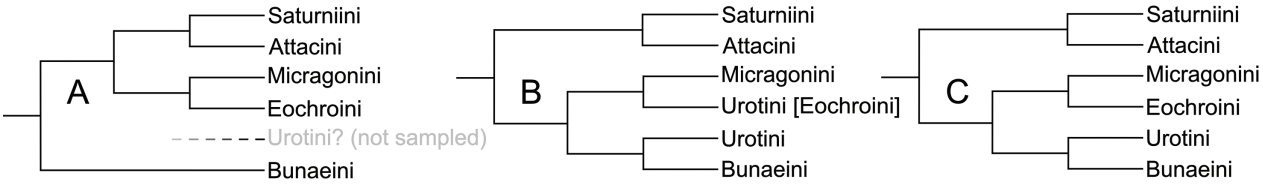

Figure 16. Topological patterns of genomic phylogenies on the family Saturniidae (part). **A** Nethavhani et al. (2022: fig. 9). **B** Regier et al. (2008: fig. 2). **C** Rougerie et al. (preprint: fig. 2).

discussions in sections 4.1–4.6, the genera *Tagoropsis*, *Pseudantheraea*, *Maltagorea* and *Sinobirma* are here considered to form a monophyletic group. The taxonomic status of *Tagoropsiella*, which occurs only on the African mainland and is close to *Tagoropsis* (Table S5), is ambiguous, and the genus is possibly a subjective synonym of *Tagoropsis*. Whether or not to distinguish this taxon does not affect the biogeographic conclusions regarding *Sinobirma*, which is why *Tagoropsiella* is here regarded as a supplementary group close to *Tagoropsis*. The currrent distribution of the genus *Sinobirma* could be explained by the following hypotheses, which are based on the distributional conditions of a most recent common ancestor of this generic group. In contrast, their current geographic distributions is not necessarily indicative of evolutionary relationships:

Hypothesis I. A Gondwanan origin of the group's ancestor, prior to India separating from Madagascar (land connection or dispersal across narrow straits still possible). After complete separation of India (straits too wide for dispersal), the ancestor present in India developed into a distinct lineage (*Sinobirma*) that arrived in Asia, whereas the individuals in Africa split into lineages on the mainland (*Tagoropsis* and *Pseudantheraea*) and Madagascar (*Maltagorea*).

Hypothesis II. After India had separated completely from Madagascar, the ancestor of *Sinobirma* originated from taxa in mainland Africa (*Tagoropsis* and *Pseudantheraea*) or Madagascar (*Maltagorea*), followed by expansion to Asia (*Sinobirma*) and extinction in Africa.

Hypothesis III. The common ancestor originated on the Eurasian Plate, or the insular India (completely separated from Madagascar), or formed after the two land masses collided, giving rise to the Asian lineage (*Sinobirma*) and dispersing to mainland Africa (*Tagoropsis* and *Pseudantheraea*) and finally Madagascar (*Maltagorea*).

Nässig and Oberprieler (1994) considered certain similarity between the genital structures of *S. malaisei* and *M. auricolor* a potential synapomorphy. The genital structures of Saturniidae are not strongly influenced by environmental factors (climates, vegetations, natural enemies, etc.), and *Sinobirma* might have reached Asia through northern Africa or insular India, while developing relatively little change in genital structures, as in some members of the Madagascan *Maltagorea*. Consequently, these similarities between the two genera are plesiomorphic traits retained by chance. This would fit to both hypotheses I and II.

Immature stages of the family Saturniidae make up the longest part of the lifecycle, and larval habitus and behavioral features are particularly influenced by evolutionary pressures linked to the biotopes they occur in. Firstly, the immatures of *Pseudantheraea* and *Maltagorea* each of features that are unique within the group of genera, while *Tagoropsis* and *Sinobirma* share fairly visible, similar characteristics, i.e., in morphology and biology of larvae and pupae. These shared features are unlikely to have evolved convergently, and the sharing of homologous characteristics indicates that the historical habitat of *Sinobirma* was probably more similar to the one of *Tagoropsis*.

Secondly, both *Pseudantheraea* and *Tagoropsis* occur on the African continent in adjacent or partially overlapping habitats (Fig. 17), yet, their dominating adaptive characteristics of immatures are divergent. With the evolutionary diversification of *Maltagorea* on the island of Madagascar in mind, it seems reasonable to assume a similar diversification for *Sinobirma* if it had drifted on an insular India. One would expect more autapomorphies in the immature stages, which is not case as described in this paper. Consequently, these immature characteristics are only in agreement with one evolutionary hypothesis, namely hypothesis II.

Considering the extensive distribution of Urotini and its sister tribe Bunaeini in Africa (see section 4.6), these African taxa and *Sinobirma* seem unlikely to be of shared Asian origin, rendering hypothesis III unrealistic. The Himalayas have been central to the evolution of most Asian saturniid genera/subgenera except *Perisomena* Walker, 1855, i.e., the genera *Actias* Leach, 1815, *Antheraea* Hübner, 1819, *Telea* Hübner, 1819, *Antheraeopsis* Wood-Mason, 1886, *Cricula* Walker, 1855, *Lemaireia* Nässig & Holloway, 1988, *Rinaca* Walker, 1855, *Cachosaturnia* Naumann, Löffler & Näss-sig, 2012, *Saturnia* Schrank, 1802, *Neoris* Moore, 1862, *Loepa* Moore, 1859, *Attacus* Linnaeus, 1767, *Archaeoattacus* Watson, 1914, *Samia* Hübner, 1819, *Rhodinia* Staudinger, 1892, *Solus* Watson, 1913, *Salassa* and *Aglia* Ochsenheimer, 1810. These genera have all a wider subtropical and tropical Asian, temperate palearctic or even New World distribution. In contrast, *Sinobirma* is a relict taxon with a distribution restricted to the northeastern corner of the Indian plate.

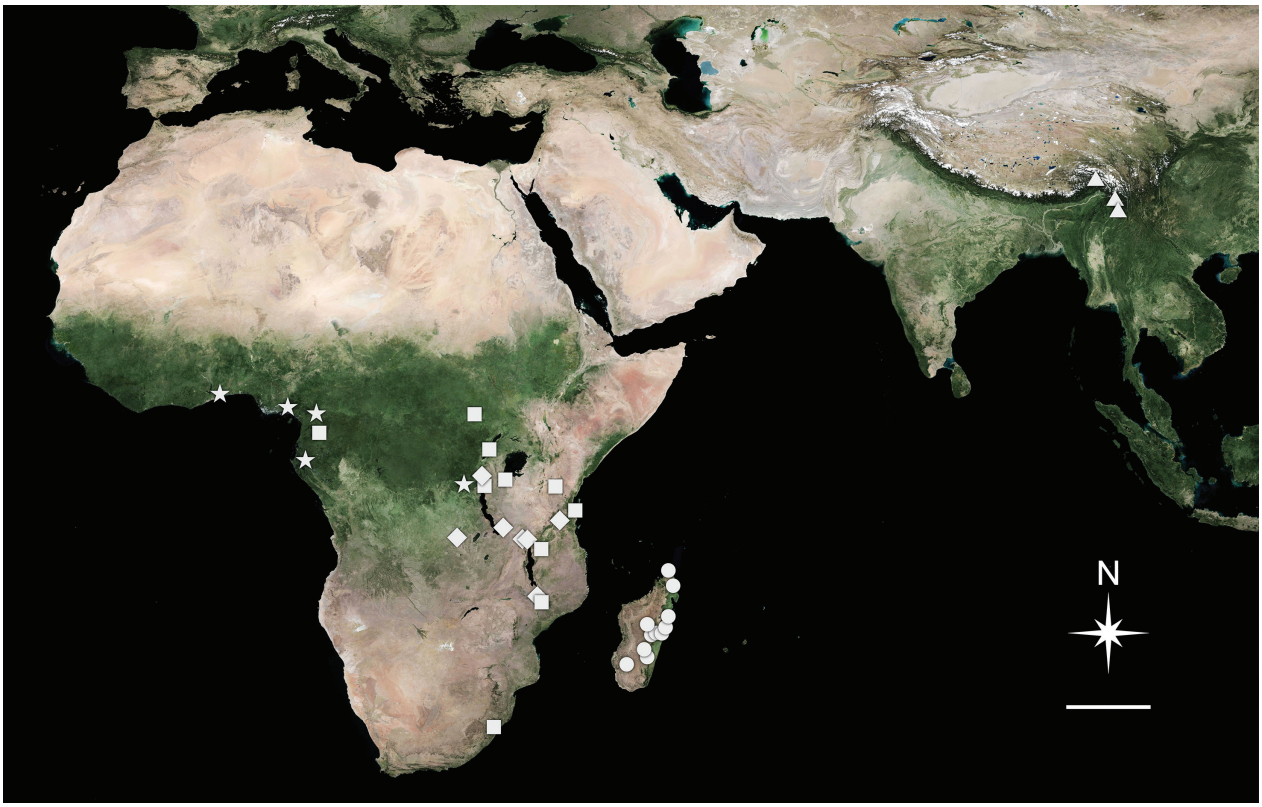

Figure 17. World satellite map (Anonymous 2022) showing the distribution of the type-localities (Table S5) of species within the monophyletic clade that includes *Tagoropsis* (squares), *Pseudantheraea* (stars), *Maltagorea* (circles) and *Sinobirma* (triangles). Scale bar = 1000 km.

5. Conclusions

This paper discussed the life history and related biological characteristics of the genus *Sinobirma*, leading to the really central questions of how and when *Sinobirma* separated phylogenetically and geographically from its closest relatives in Africa. Multiple characteristics strongly support hypothesis II (section 4.7), i.e., that the ancestor of *Sinobirma* arrived in Asia by dispersal, rather than by continental drift as favoured by Nässig and Oberprieler (1994). From the perspective of the current geographic distribution of this group, Himalayan *Sinobirma* and Madagascan *Maltagorea* are examples of peripatric or allopatric speciations, while continental African *Tagoropsis* and *Pseudantheraea* originated more likely through parapatric or sympatric speciation.

Relative to the other two genera, immature stages of *Tagoropsis* and *Sinobirma* share more morphological and biological similarities, which is here considered to be key for clarifying the dispersal history of the latter. However, this does not mean that *Tagoropsis* and *Sinobirma* are sister taxa in a phylogenetic sense, because it isn't clear at present to what extent these traits are shared ancestral or derived characteristics.

The host preference experiment demonstrated that although larvae died quickly in L_1 after feeding on some hosts, the feeding behavior of the early larva of the genus *Sinobirma* can be triggered by many different Himalayan plants within different families. This potential to exploit a broad range of plants might have enabled moths to expand their populations without the constraints caused by monophagy and the distribution of a specific host plant. Consequently, these larvae are well equipped to continuously discover and adapt to new, suitable host plants in natural environments in a relatively short time, as might be expected during dispersal. Considering that *Tagoropsis*, *Pseudantheraea* and *Maltagorea* all utilize a much broader range of host plants, this may indicate that their most recent common ancestor might have been polyphagous.

Before reaching today's southeastern Himalayas, whether through Europe, the Middle East or both, the northwestern Indian subcontinent was obviously the logical dispersal route for the ancestors of *Sinobirma*. None of these areas is home to the four genera today, only a distantly related *Usta* species occurs on the dry Arabian Peninsula (Nässig et al. 2015). In contrast, the humid areas of similar altitude in the southeastern Himalayas (including central Yunnan) of the Indochinese Peninsula are well suited to the reproduction of *Sinobirma*. However, as the genus also has not been widely reported in these regions, a more plausible explanation might be that the genus is currently colonizing these areas, rather than that more widespread populations in southeastern Asia have become extinct. This is another reason why this paper doesn't consider the reversible evolutionary route (hypothesis III in the section 4.7) to be likely.

Genomic research by Rougerie et al. (preprint) demonstrated that *Sinobirma* dispersed from Africa to the Oriental region in the middle Miocene (ca. 14 Mya), whereas *Maltagorea* colonized Madagascar from the African continent at a similar time (ca. 12 Mya). According to Zhang et al. (2014), northern Africa and western Asia were relatively wetter than today during the late Oligocene to early Miocene, while middle (Henrot et al. 2017) and late Miocene (Pound et al. 2011) may also have been similar. Such climatic conditions would have supported dispersal across the three continents and around proto-Mediterranean and Tethys-Paratethys coasts by more saturniids.

Rougerie et al. (preprint) already mentioned that the dispersals by *Epiphora* Wallengren, 1860, *Eosia* Le Cerf, 1911, and *Argema* Wallengren, 1858 occurred from Asia to the Africa (ca. 14 Mya), almost synchronous with the divergence of *Sinobirma* from its African relatives. This might mean that their ancestors all encountered a common historical event in the same region, most likely aridification. This might have increasingly restricted distributions to relatively wet areas, separating populations.

Opinions differ on when the Sahara and Arabian deserts formed. Schuster et al. (2006) stated that the onset of recurrent desert conditions in the Sahara started at least 7 Mya (Miocene), but Kroepelin (2006) soon added that "previous studies suggest that the climate during most of the Miocene was relatively humid and that the first appearance of persistent and widespread arid conditions occurred during the Pliocene". In contrast, Zhang et al. (2014) hypothesized that during the late Miocene epoch (ca. 11–7 Ma, Tortonian), the shrinking of the Tethys Sea weakened the African summer monsoon and caused the expansion of the desert in these areas. Furthermore, Pleistocene glaciation (e.g., Ehlers and Gibbard 2008) might have directly affected or extirpated a historical European population of *Sinobirma* (if it ever existed), possibly forcing survivors to disperse into the more ecologically favorable southeastern direction (Indian subcontinent).

In the superfamily Bombycoidea, another Sub-Himalayan taxon *Tibetanja* Naumann, Nässig & Rougerie, 2020 (Eupterotidae) may have the same distributional pattern and dispersal history as the saturniid genus *Sinobirma*. The former is probably the only Asian genus of the African subfamily Janinae (Eupterotidae) (Naumann and Nässig 2022).

In any case, it is necessary to explore the immature characteristics of more members of the genera *Tagoropsis*, *Pseudantheraea* and *Maltagorea*, as well as of *S. malaisei* and *S. myanmarensis* to further refine our understanding of the evolution of the genus *Sinobirma*.

6. Acknowledgments

I am most sincerely grateful to Richard S. Peigler (University of the Incarnate Word, San Antonio) for his guidance and help in my studies of Saturniidae in recent years. He provided much literature and valuable advice, as well as editing the English for this article. Rodolphe Rougerie (Muséum National d'Histoire naturelle, Paris) is one of the few people who has personally traveled to the natural habitat of *Sinobirma* to study the genus, and I thank him for providing references and reviewing my manuscript. Andreas Zwick (Commonwealth Scientific and Industrial Research Organisation, Canberra) helped with advice and editing the manuscript. Michel J. Faucheux (Faculté des Sciences et des Techniques, Nantes) shared with me knowledge about sensilla. Finally, special thanks go to Yanqun Liu (Shenyang Agricultural University, Shenyang) and Dasong Chen (Institute of Zoology, Guangdong Academy of Science, Guangzhou), who assisted in genomic data analyses and reviewed the relevant paragraphs.

7. References

Adès D (2007) Note sur la fluorescence des cocoons dans les élevages d'Actien. Hybride d'Actien *Actias* [*sinensis* male × *dubernardi* femelle]: Un exemple de fluorescence composite. Lambillionea 107(1): 36–43.

Anonymous (2022) MAP WORLD: GS(2022)3124. https://www.tianditu.gov.cn

Austin AD, Johnson NF, Dowton M (2005) Systematics, evolution, and biology of scelionid and platygastrid wasps. Annual Review of Entomology 50: 553–582. https://doi.org/10.1146/annurev.ento.50.071803.130500

Basquin P (2015) Contribution à la connaissance de *Maltagorea auricolor* Mabille de Madagascar (Lepidoptera, Saturnnidae). Saturnafrica 21: 3–15, pls. 1–5.

Basquin P, Rougerie R (2009) Contribution à la connaissance du genre *Maltagorea* Bouyer, 1993: description d'une nouvelle espèce révélée par la combinaison de caractères morphologiques et de codes barres ADN (Lepidoptera, Saturniidae). Bulletin de la Société entomologique de France, 114(3): 257–263. https://doi.org/10.3406/bsef.2009.2732

Bouvier E-L (1928) Faune des Colonies Françaises, Tome 2, Fasc. 5: Les Saturnioïdes de l'Afrique tropicale française. Société d'Éditions Géographiques, Maritimes et Coloniales, Paris, 267 pp. [pp. 449–715], 6 pls.

Bouvier E-L (1936) Mémoirs du Muséum National d'Histoire naturelle (Nouvelle Série), Tome 3, Étude des Saturnioïdes normaux: Famille des Saturniidés. Éditions du Muséum, Paris, 354 pp., 12 pls.

Bouyer T (1993) *Maltagorea* n. gen., un nouveau genre de Saturniidae malgache (Lepidoptera: Saturniidae, Saturniinae, Pseudapheliini). Lambillionea 93(1): 97–102.

Bouyer T, Lampe REJ, Nässig WA (2004) The life history of *Pseudantheraea discrepans* (Butler, 1878), with an ecological comparison with *P. imperator* Rougeot, 1962 (Lepidoptera: Saturniidae, Saturniinae, Urotini). Nachrichten des Entomologischen Vereins Apollo 25(1/2): 27–37.

Bryk F (1944) Entomological results from the Swedish expedition 1934 to Burma and British India. Lepidoptera: Saturniidae, Bombycidae, Eupterotidae, Uraniidae, Epiplemidae und Sphingidae, gesammelt von René Malaise. Arkiv för Zoologi 35A(8): 1–55, 1–6 pls.

Chandra K, Kumar V, Singh N, Raha A, Sanyal AK (2019) Assemblages of Lepidoptera in Indian Himalaya through long term monitoring plots. Zoological Survey of India, Kolkata, 457 pp.

Chen MM, Li Y, Chen M, Wang H, Li Q, Xia RX, Zeng CY, Li YP, Liu YQ, Qin L (2014) Complete mitochondrial genome of the atlas moth, *Attacus atlas* (Lepidoptera: Saturniidae) and the phylogenetic relationship of Saturniidae species. Gene 545(1): 95–101. https://doi.org/10.1016/j.gene.2014.05.002

Cooper MR (2002) Notes on classification. In: Cooper MR, Cooper MD (Eds) The Emperor Moths of KwaZulu-Natal. Peroniceras Press, New Germany, x–xvi.

Cooper MR, Cooper MD (2002) The Emperor Moths of KwaZulu-Natal. Peroniceras Press, New Germany, xvi + 103 pp.

Crotch WJB (1956) A Silkmoth Rearer's Handbook. The Amateur Entomologists' Society, London, 165 pp., 26 pls.

d'Abrera B (2012) Saturniidae Mundi: Saturniid Moths of the World. Part 2. Goecke & Evers, Keltern, xlix + 178 pp.

Donath A, Jühling F, Al-Arab M, Bernhart SH, Reinhardt F, Stadler PF, Middendorf M, Bernt M (2019) Improved annotation of protein-coding genes boundaries in metazoan mitochondrial genomes. Nucleic Acids Research 47(20): 10543–10552. https://doi.org/10.1093/nar/gkz833

Ehlers J, Gibbard P (2008) Extent and chronology of Quaternary glaciation. Episodes, Journal of International Geoscience 31(2): 211–218. https://doi.org/10.18814/epiiugs/2008/v31i2/004

Ferguson DC (1972) The Moths of America, North of Mexico, Fascicle 20.2B, Bombycoidea: Saturniidae (Part). The Curwen Press, London, 1 + 121 + vii pp. [1+ pp. 155–275 + pp. xv–xxi], 11 pls. [pls. 12–22].

Gardiner BOC (1982) The Amateur Entomologist Vol. 12: A Silkmoth Rearer's Handbook (3rd Edition). The Amateur Entomologists' Society, London, xiii + 255 pp., 58 pls.

Goulet H, Huber JT (Eds) (1993) Hymenoptera of the World: An Identification Guide to Families. Centre for Land and Biological Resources Research, Ottawa, vii + 668 pp.

Greiner S, Lehwark P, Bock R (2019) OrganellarGenomeDRAW (OGDRAW) version 1.3.1: expanded toolkit for the graphical visualization of organellar genomes. Nucleic Acids Research 47: W59–W64.

Griveaud P (1961) Faune de Madagascar 14: Insects: Lépidoptères Eupterotidae et Attacidae. L'Institut de Recherche Scientifique de Madagascar, Antananarivo, 64 pp., 12 pls.

Henrot AJ, Utescher T, Erdei B, Dury M, Hamon N, Ramstein G, Krapp M, Herold N, Goldner A, Favre E, Munhoven G, François L (2017) Middle Miocene climate and vegetation models and their validation with proxy data. Palaeogeography, Palaeoclimatology, Palaeoecology 467: 95–119. https://doi.org/10.1016/j.palaeo.2016.05.026

Hoang DT, Chernomor O, von Haeseler A, Minh BQ, Vinh LS (2018) UFBoot2: Improving the ultrafast bootstrap approximation. Molecular Biology and Evolution 35(2): 518–522. https://doi.org/10.1093/molbev/msx281

Hoekstra JM, Molnar JL, Jennings M, Revenga C, Spalding MD, Boucher TM, Robertson JC, Heibel TL, Ellison K (2010) The Atlas of Global Conservation: Changes, Challenges, and Opportunities to Make a Difference. University of California Press, Berkeley-Los Angeles, xiv + 234 pp.

Holland WJ (1892) Notes upon the transformations of some African Lepidoptera. Psyche, a journal of entomology 6: 213–216, pl. 5.

Jiang ST, Hong GY, Yu M, Li N, Yang Y, Liu YQ, Wei ZJ (2009) Characterization of the complete mitochondrial genome of the giant silkworm moth, *Eriogyna pyretorum* (Lepidoptera: Saturniidae). International Journal of Biological Sciences 5(4):351–365. https://doi.org/10.7150/ijbs.5.351

Kalyaanamoorthy S, Minh BQ, Wong TKF, von Haeseler A, Jermiin LS (2017) ModelFinder: fast model selection for accurate phylogenetic estimates. Nature Methods 14: 587–589. https://doi.org/10.1038/nmeth.4285

Katoh K, Rozewicki J, Yamada KD (2019) MAFFT online service: multiple sequence alignment, interactive sequence choice and visualization. Briefings in Bioinformatics 20(4): 1160–1166.

Kitching IJ, Rougerie R, Zwick A, Hamilton CA, St Laurent RA, Naumann S, Mejia LB, Kawahara AY (2018) A global checklist of the Bombycoidea (Insecta: Lepidoptera). Biodiversity Data Journal 6: e22236. https://doi.org/10.3897/BDJ.6.e22236

Kim MJ, Park JS, Kim H, Kim SR, Kim SW, Kim KY, Kwak W, Kim I (2022) Phylogeographic relationships among *Bombyx mandarina* (Lepidoptera: Bombycidae) populations and their relationships to *B. mori* inferred from mitochondrial genomes. Biology (Basel) 11(1): 68. https://doi.org/10.3390/biology11010068

Kroepelin S (2006) Revisiting the age of the Sahara Desert. Science 312(5777): 1138–1139. https://doi.org/10.1126/science.312.5777.1-138b

Kumar S, Stecher G, Li M, Knyaz C, Tamura K (2018) MEGA X: molecular evolutionary genetics analysis across computing platforms. Molecular Biology and Evolution 35(6): 1547–1549. https://doi.org/10.1093/molbev/msy096

Lampe REJ (2010) Saturniidae of the World (Pfauenspinner der Welt). Verlag Dr. Friedrich Pfeil, München, 368 pp.

Langley J, van der Westhuizen S, Morland G, van Asch B (2020) Mitochondrial genomes and polymorphic regions of *Gonimbrasia belina* and *Gynanisa maja* (Lepidoptera: Saturniidae), two important edible caterpillars of Southern Africa. International Journal of Biological Macromolecules 144: 632–642. https://doi.org/10.1016/j.ijbiomac.2019.12.055

Lautenschläger T, Neinhuis C, Monizi M, Mandombe JL, Förster A, Henle T, Nuss M (2017) Edible insects of northern Angola. African Invertebrates 58(2): 55–82. http://doi.org/10.3897/AfrInvertebr.58.21083

Liu ZY (2023) An "American" silkmoth endemic to Himalayas, part I: life history and natural distribution of *Antheraea compta* Rothschild, 1899 (Lepidoptera, Saturniidae). Deutsche Entomologische Zeitschrift 70(2): 261–282. https://doi.org/10.3897/dez.70.102952

Liu ZY, Peigler RS (2021) The life history and entomophagy of *Saturnia centralis* and related Saturniidae. Journal of the Lepidopterists' Society 75(3): 174–186. https://doi.org/10.18473/lepi.75i3.a2

Mabossy-Mobouna G, Ombeni JB, Bouyer T, Latham P, Bisaux F, Bocquet E, Brinck B, Mbuta AKK, Madamo-Malasi F, Ngoie LN, Eckebil PPT, Malaisse F (2022) Diversity of edible caterpillars and their host plants in the Republic of the Congo. African Journal of Tropical Entomology Research 1(1): 3–27. https://doi.org/10.5281/zenodo.6351855

Meister F (2011) A Guide to the Breeding of Tropical Silk Moths (Lepidoptera: Saturniidae). Verlag Dr. Friedrich Pfeil, München, 220 pp.

Min TL, Brach AR (2008) Coriariaceae. In: Wu ZY, Raven PH, Hong DY (Eds) Flora of China. Vol. 11 (Oxalidaceae through Aceraceae). Science Press, Beijing, Missouri Botanical Garden Press, St. Louis, 333–334.

Moskowitz D (2018) Hunting caterpillars with a UV flashlight – part 2. News of the Lepidopterists' Society 60(4): 169–171.

Moskowitz D (2021) Foiling crypsis: surveying Lepidoptera caterpillars with UV light. Entomologist's Monthly Magazine 157: 9–16.

Nässig WA, Oberprieler RG (1994) Notes on the systematic position of *Sinobirma malaisei* (Bryk 1944) and the genera *Tagoropsis*, *Maltagorea*, and Pseudantheraea (Lepidoptera, Saturniidae: Saturniinae, Pseudapheliini). Nachrichten des Entomologischen Vereins Apollo 15(3): 369–382.

Nässig WA, Naumann S, Oberprieler RG (2015) Notes on the Saturniidae of the Arabian Peninsula, with description of a new species (Lepidoptera: Saturniidae). Nachrichten des Entomologischen Vereins Apollo 36 (1): 31–38.

Naumann S, Nässig WA (2022) Distributional note on *Tibetanja tagoroides* Naumann et al., 2020 (Lepidoptera, Eupterotidae, Janinae): Additional locality records. Nachrichten des Entomologischen Vereins Apollo 43 (2): 102–103.

Naumann S, Smetacek P (2023) Eleven new Saturniidae species from India and adjacent countries. Bionotes 25 (3): 49–90.

Nethavhani Z, Straeuli R, Hiscock K, Veldtman R, Morton A, Oberprieler RG, van Asch B (2022) Mitogenomics and phylogenetics of twelve species of African Saturniidae (Lepidoptera). PeerJ 10: e13275. http://doi.org/10.7717/peerj.13275

Nguyen LT, Schmidt HA, von Haeseler A, Minh BQ (2015) IQ-TREE: A fast and effective stochastic algorithm for estimating maximum likelihood phylogenies. Molecular Biology and Evolution 32(1): 268–274. https://doi.org/10.1093/molbev/msu300

Oberprieler RG (1997) Classification of the African Saturniidae (Lepidoptera), the quest for natural groups and relationships. Metamorphosis, Journal of the Lepidopterists' Society of Africa, Occasional Supplement 3: 142–155.

Oberthür C (1916) Suite de la révision des espèces nouvelles des Lépidoptères malgaches. Études de Lépidoptérologie comparée 11: 247–262, pls. 370–372.

Packard AS (1914) Memoirs of the National Academy of Sciences 12 (1st Memoir): Monograph of the Bombycine Moths of North America, Including Their Transformations and Origin of the Larval Markings and Armature. Part 3. Families Ceratocampidae (Exclusive of Ceratocampinae), Saturniidae, Hemileuciidae, and Brahmaeidae (Edited by Cockerell TDA). National Academy of Sciences, Washington, ix + 516 pp., 113 pls.

Paulian R (1953) Récherches sur les Insectes d'importance biologique à Madagascar, XII à XX XIV *Copaxa subocellata* BUTLR. (Lép. Saturn.). Mémoires de l'Institut Scientifique de Madagascar Série E. Entomologie 3(3): 15–17.

Peel MC, Finlayson BL, McMahon TA (2007) Updated world map of the Köppen-Geiger climate classification. Hydrology and Earth System Sciences 11: 1633–1644. https://doi.org/10.5194/hess-11-1633-2007

Peigler, RS (1999) Book review: Saturniidae Mundi: saturniid months of the world, part 3, by Bernard d'Abrera. Journal of the Lepidopterists' Society 53(1): 48.

Pinhey ECG (1956) The emperor moths of eastern Africa. Journal of The East Africa Natural History Society 23(1): 1–62.

Pinhey ECG (1972) Emperor Moths of South and South-Central Africa. C. Struik (Pty) Ltd., Cape Town. xi + 150 pp., 43 pls.

Platt EE (1921) List of foodplants of some South African lepidopterous larvae. South African Journal of Natural History 3(1): 65–138.

Pound MJ, Haywood AM, Salzmann U, Riding JB, Lunt DJ, Hunter SJ (2011). A Tortonian (late Miocene, 11.61–7.25 Ma) global vegetation reconstruction. Palaeogeography, Palaeoclimatology, Palaeoecology 300: 29–45. https://doi.org/10.1016/j.palaeo.2010.11.029

Prjibelski A, Antipov D, Meleshko D, Lapidus A, Korobeynikov A (2020) Using SPAdes de novo assembler. Current protocols in bioinformatics 70(1): e102. https://doi.org/10.1002/cpbi.102

Racheli L, Racheli T (2006) Phylogenetic hypothesis and classification: theoretical and methodological issues with reference to some studies on Saturniidae (Lepidoptera: Saturniidae). SHILAP Revista de lepidopterología 34(133): 5–12.

Regier JC, Grant MC, Mitter C, Cook CP, Peigler RS, Rougerie R (2008) Phylogenetic relationships of wild silkmoths (Lepidoptera: Saturniidae) inferred from four protein-coding nuclear genes. Systematic Entomology 33(2): 219–228. https://doi.org/10.1111/j.1365-3113.2007.00416.x

Rondot N (1887) L'art de la soie: les soies (2nd Edition). Tome 2. Impremerie Nationale, Paris, 604 pp.

Rougeot P-C (1949) Description des stades post-embryonnaires de quelques saturnioides Gabonais. Bulletin mensuel de la Société Linnéenne de Lyon 18(10): 208–217.

Rougeot P-C (1950) Description d'une nouvelle espèce de Saturniide du Gabon et de ses premiers états. Bulletin mensuel de la Société linnéenne de Lyon 19(10): 224–227.

Rougeot P-C (1955) Encyclopédie entomologique 34: Les Attacidés (Saturnidae) [sic] de l'Équateur africain français. Paris, Editions Paul Lechevalier, Paris, 116 pp., 12 pls.

Rougeot P-C (1962) Initations Africaines 14: Les Lépidoptères de l'Afrique noire occidentale, Fascicule 4, Attacidés (= Saturniidés). Institut Français d'Afrique Noire, Dakar, 214 pp.

Rougerie R (2003) Re-capture of *Sinobirma malaisei* in China: description of the female genitalia and comments on the systematic position of the genus in the tribe Urotini (Saturniidae). Nota lepidopterologica 25(4): 227–233.

Rougerie R (2005) Phylogénie et biogéographie des Saturniinae (Lepidoptera: Bombycoidea, Saturniidae). Approche morphologique et moléculaire. PhD Thesis, Muséum National d'Histoire naturelle, Paris, France. 530 pp., 45 pls., CD-R

Rougerie R, Estradel Y (2008) Morphology of the preimaginal stages of the African emperor moth *Bunaeopsis licharbas* (Maassen and Weyding): Phylogenetically informative characters within the Saturniinae (Lepidoptera: Saturniidae). Journal of Morphology 269(2): 207–232. https://doi.org/10.1002/jmor.10562

Rougerie R, Naumann S, Nässig WA (2012) Morphology and molecules reveal unexpected cryptic diversity in the enigmatic genus *Sinobirma* Bryk, 1944 (Lepidoptera: Saturniidae). Plos One 7(9): e43920. https://doi.org/10.1371/journal.pone.0043920

Rougerie R, Cruaud A, Arnal P, Ballesteros-Mejia L, Condamine FL, Decaëns T, Elias M, Gey D, Hebert PDN, Kitching IJ, Lavergne S, Lopez-Vaamonde C, Murienne J, Cuenot Y, Nidelet S, Rasplus JY (preprint) Phylogenomics Illuminates the Evolutionary History of Wild Silkmoths in Space and Time (Lepidoptera: Saturniidae). bioRxiv: 2022.03.29.486224. https://dx.doi.org/10.1101/2022.03.29.486224

Santin A (2004) Répertoire des Plantes-Hôtes de Substitution des chenilles du monde. Éléments recueillis dans des publications entomologiques et résultats d'expérimentations personnelles (2nd Edition). Office pour l'information éco-entomologique, Guyancourt, 1228 pp.

Schultze A (1914) Zur Kenntnis der ersten Stände von einigen west- und zentralafrikanischen Heteroceren. Archiv für Naturgeschichte (A) 80(1): 144–163, pls. 1–3.

Schuster M, Duringer P, Ghienne JF, Vignaud P, Mackaye HT, Likius A, Brunet M (2006) The age of the Sahara Desert. Science 311(5762): 821. https://doi.org/10.1126/science.1120161

Scott AW (1890) Australian Lepidoptera and Their Transformations, by the Late Alexander Walker Scott, with Illustrations Drawn from Life by His Daughters, Harriet Morgan and Helena Forde. Volume 2 (Edited and Revised by Olliff AS and Forde H). Australian Museum, Sydney, 36 pp., 12 pls.

Seydel C (1939) Contribution à l'étude de la biologie de la faune entomologique éthiopienne. In: Jordan K, Hering EM (Eds) Verhandlungen Band 2. VII. Internationaler Kongress für Entomologie. G. Uschmann, Weimar, 1308–1330, pls. 149–156.

Sondhi S, Sondhi Y, Roy P, Kunte K (2021a) Moths of India, v. 2.71. Indian Foundation for Butterflies. https://www.mothsofindia.org

Sondhi S, Karmakar T, Sondhi Y, Kunte K (2021b) Moths of Tale Wildlife Sanctuary, Arunachal Pradesh, India with seventeen additions to the moth fauna of India (Lepidoptera: Heterocera). Tropical Lepidoptera Research 31 (Supplement 2): 1–53. https://doi.org/10.5281/zenodo.5062572

Song SY, Wang PX (2013) Tibet Climate. China Meteorological Press, Beijing. vi + 492 pp. [in Chinese with English subtitle]

Staude HS, Mecenero S, Oberprieler RG, Sharp A, Sharp I, Williams MC, Maclean M (2016) Supplementary material to: An illustrated report on the larvae and adults of 962 African Lepidoptera species. Results of the Caterpillar Rearing Group: a novel, collaborative method of rearing and recording lepidopteran life-histories. Metamorphosis 27 (CRG Supplement): S1–S330.

Stone SE (1991) Memoir Number 4: Foodplants of World Saturniidae. The Lepidopterists' Society, xv + 186 pp., 1 pl.

Vårdal H, Taeger A (2011) The life of René Malaise: from the wild east to a sunken island. Zootaxa 3127: 38–52. https://doi.org/10.11646/zootaxa.3127.1.2

Vinciguerra R, Racheli L (2005) A further record of *Sinobirma malaisei* (Bryk, 1944) from Myanmar (Lepidoptera: Saturniidae: Saturniinae). Beitrage zur Kenntnis der wilden Seidenspinner 3(1): 46–48.

Wagner DL, Nall B (2022) *Syssphinx* larvae of the lower Rio Grande Valley of Texas with emphasis on the life history of *Syssphinx tamaulipasiana*. Journal of the Lepidopterists' Society 76(2): 135–139. https://doi.org/10.18473/lepi.76i2.a5

Wolfe JA (1979) Temperature Parameters of Humid to Mesic Forests of Eastern Asia and Relation to Forests of Other Regions of the Northern Hemisphere and Australasia. Geological Survey Professional Paper 1106. United States Government Printing Office, Washington, iii + 37 pp., 3 pls.

Zhang JW, Chen WL, Zhao KY, Wang JT, Li BS (1988) Chapter 15, vegetation division of Xizang, section 3, vegetation division. In: Zhang JW (Ed). The Series of the Scientific Expedition to the Qinghai-Xizang Plateau: Vegetation of Xizang (Tibet). Science Press, Beijing, 262–330 [in Chinese with English subtitles].

Zhang WW (2012) Searching for the Sino-Myanmar silkmoth. Outdoor Exploration 124: 124–129. [in Chinese with English subtitle]

Zhang WW, Li YS (2011) Chinese Insects Illustrated. Chongqing University Press, Chongqing. 691 pp. [in Chinese with English subtitle]

Zhang ZS, Ramstein G, Schuster M, Li C, Contoux C, Yan Q (2014) Aridification of the Sahara Desert caused by Tethys Sea shrinkage during the Late Miocene. Nature 513: 401–404. https://doi.org/10.1038/nature13705

Zheng LL, Dong H, Geng QR, Liao GY, Lou XY, Li S, Sun ZM (2018) Regional Geological Survey Report of the People's Republic of China (1:250000), Mêdog County (H46 C 003004). Geological Publishing House, Beijing. iv + 310 pp., 1 folding map (with instruction). [in Chinese]

Supplementary Material 1

Tables S1–S3, S5, S6

Authors: Liu ZY (2024)
Data type: .xlsx
Explanation notes: Table S1. Individual numbers of *Sinobirma bouyeri* in different developmental stages, fed on *Coriaria nepalensis* (group A, in green bars) and *Prunus cerasoides* (group B, in red bars), respectively. — **Table S2.** Environmental monitoring data for the habitat of *Sinobirma bouyeri* (Mêdog County, Tibet, 2134 m) — **Table S3.** Circadian rhythm of *Sinobirma bouyeri* L_5. — **Table S5.** Taxonomic checklist of *Sinobirma* and its close relatives. — **Table S6.** Inventory of DNA sequences used in this paper.

Link: https://doi.org/10.3897/asp.82.e104232.suppl1

Supplementary Material 2

Table S4

Authors: Liu ZY (2024)
Data type: .pdf
Explanation notes: Pupal data of *Sinobirma bouyeri* raised on *Coriaria nepalensis* and *Prunus cerasoides*.

Link: https://doi.org/10.3897/asp.82.e104232.suppl2

Supplementary Material 3

File S1

Authors: Liu ZY (2024)
Data type: .mov
Explanation notes: Gregarious behavior of fresh *Sinobirma bouyeri* L_1.

Link: https://doi.org/10.3897/asp.82.e104232.suppl3